Geological Society of America Memoirs

Low-initial-Sr felsic plutons of the northwestern Peninsular Ranges batholith, southern California, and the role of mafic-felsic magma mixing in continental crust formation

Benjamin L. Clausen, Douglas M. Morton, Ronald W. Kistler and Cin-Ty A. Lee

Geological Society of America Memoirs 2014;211;317-344
doi: 10.1130/2014.1211(08)

The Geological Society of America
Memoir 211
2014

Low-initial-Sr felsic plutons of the northwestern Peninsular Ranges batholith, southern California, and the role of mafic-felsic magma mixing in continental crust formation

Benjamin L. Clausen*
Geoscience Research Institute and Department of Earth and Biological Sciences, Loma Linda University, Loma Linda, California 92350, USA

Douglas M. Morton*
U.S. Geological Survey and Department of Earth Sciences, University of California, Riverside, California 92521, USA

Ronald W. Kistler*
U.S. Geological Survey, 345 Middlefield Road, Menlo Park, California 94025, USA

Cin-Ty A. Lee*
Department of Earth Science, Rice University, Houston, Texas 77005, USA

ABSTRACT

We studied the formation of low-initial-Sr felsic plutons by using data from the Early Cretaceous western Peninsular Ranges batholith near Escondido, California. The systematically sampled Escondido plutons have a uniformly low initial $^{87}Sr/^{86}Sr$ isotope ratio of $Sr_i < 0.704$, but a wide range of SiO_2 compositions, from 46 to 78 wt%, which fall in three distinct groups: 20% gabbros, 35% tonalites, and 45% granodiorites. These low-Sr_i plutons are unique in having undergone one cycle of mantle melting to give basalt composition rocks, and a second cycle of arc basalt melting to give a range of SiO_2 plutons, but no third cycle of melting and contamination by old continental crust to yield high-Sr_i rocks. After doing two-cycle partial melting and fractional crystallization calculations, it was recognized that mixing of gabbro and granodiorite magmas was necessary to yield the tonalites. The linear data pattern on Harker diagrams is interpreted as resulting from mixing of mafic magma from partial melting of the mantle and felsic magma from partial melting of the lower crust to form intermediate magma. These plutons provide a simplified two-cycle Phanerozoic example of the petrogenetic process for forming continental crust.

*E-mails: bclausen@llu.edu; douglasmmorton@gmail.com; rkistler@usgs.gov; ctlee@rice.edu.

Clausen, B.L., Morton, D.M., Kistler, R.W., and Lee, C.-T.A., 2014, Low-initial-Sr felsic plutons of the northwestern Peninsular Ranges batholith, southern California, and the role of mafic-felsic magma mixing in continental crust formation, *in* Morton, D.M., and Miller, F.K., eds., Peninsular Ranges Batholith, Baja California and Southern California: Geological Society of America Memoir 211, p. 317–344, doi:10.1130/2014.1211(08). For permission to copy, contact editing@geosociety.org.

INTRODUCTION

Very few Phanerozoic arc plutons are low in initial $^{87}Sr/^{86}Sr$ ratios (Sr_i) yet high in SiO_2 concentrations. Formation of the relatively rare low-Sr_i and high-SiO_2 plutons in the northwestern Peninsular Ranges batholith of southern California are studied here in their relation to low-Sr_i and low-SiO_2 primitive basalts and high-Sr_i and high-SiO_2 mature arc granitoids in the rest of the northern Peninsular Ranges batholith and elsewhere, as summarized in Table 1.

This report on the low-Sr_i plutons of the northwestern Peninsular Ranges batholith first describes past work and sample analyses. Next, geochemical data are used to confirm that calc-alkaline magmatism occurred at a shallow level with volcanic-arc basalts and no contamination from continental crust. Two-cycle differentiation calculations for partial melting and fractional crystallization are then performed for comparison with the range of SiO_2 composition data. A discussion is included on the important role of magma mixing, the results of mass balance calculations, and an application to continental crust formation. Finally, a petrogenetic scenario is outlined for these processes.

PENINSULAR RANGES BATHOLITH

Numerous research projects have studied the tectonics, geochemistry, and geophysics of the Peninsular Ranges batholith.

TABLE 1. SUMMARY OF IGNEOUS ROCKS BASED ON Sr_i and SiO_2 CONTENT

First cycle	$Sr_i < 0.704$	$SiO_2 < 55\%$

- Volcanic
  - Mid-ocean-ridge basalt (MORB), ocean-island basalt (OIB)
  - Island-arc basalt (IAB)—in, e.g.,
    - Scotia Sea and South Shetland Islands (Saunders and Tarney, 1984)
    - Izu-Bonin-Mariana arc (Stern et al., 2003)
    - Santiago Peak volcanics in southern California (Tanaka et al., 1984)

Second cycle	$Sr_i < 0.704$	$SiO_2 > 55\%$

- Volcanic
  - Uncontaminated island arcs (Gill, 1981)—some in
    - Philippines (DuFrane et al., 2006)
    - Aleutians (Kay et al., 1978)
    - Fiji, Tonga-Kermadec, New Britain, Marianas, Japan, Kamchatka, Kurils, South Sandwich Islands
  - Uncontaminated continental arcs—some in
    - Andes and Cascades (Grove et al., 1982; Conrey et al., 2001)
      may be extrusive equivalent of western Peninsular Ranges batholith (Lee et al., 2007)
- Plutonic
  - Precambrian plutons (Faure and Powell, 1972)—many in
    - Africa (Fitches et al., 1983)
    - Canadian Shield, basement of western United States (Ernst, 1990)
  - Anorogenic plutons—a few in
    - Oslo graben (Neumann, 1980)
    - New Hampshire (Eby et al., 1992)
    - continent-continent collision granites in the Carolinas (Fullagar and Butler, 1979)
  - Uncontaminated Phanerozoic volcanic arc plutons—a few in
    - Newfoundland (Whalen et al., 1987)
    - Japan (Kamiyama et al., 2007)
    - New Zealand (Tulloch and Kimbrough, 2003)
    - Himalayas (Mikoshiba et al., 1999)
    - Lachlan fold belt, Australia (Keay et al., 1997)
    - Pisco valley, Linga Super-unit, Coastal Batholith, Peru (Beckinsale et al., 1985)
    - Aleutians (Kay et al., 1983)
    - British Columbia (Armstrong, 1988)
    - Idaho (Armstrong et al., 1977; Fleck and Criss, 1985; Criss and Fleck, 1987)
    - Klamath Mountains (Snoke and Barnes, 2006)
    - Sierra Nevadas (Kistler and Peterman, 1978)
    - northwestern Peninsular Ranges batholith (Baird and Miesch, 1984; Langenheim et al., 2004)

Third cycle or more	$Sr_i > 0.704$	$SiO_2 > 55\%$

- Volcanic
  - Contaminated island arcs (Gill, 1981)—very common, e.g.,
    - Kamchatka, Japan, New Zealand, N. Lesser Antilles, Taiwan
- Plutonic
  - Phanerozoic plutons—most common, e.g.,
    - eastern Peninsular Ranges batholith (Baird and Miesch, 1984; Langenheim et al., 2004)

The relevant geology and major faults of the region are shown in Figure 1. Published data include major-element analyses, U-Pb, Rb-Sr, K-Ar, Sm-Nd, and $\delta^{18}O$ isotope analyses, as well as specific gravity, aeromagnetic, and seismic data. A partial summary with references was tabulated by Symons et al. (2003).

The most prominent geochemical feature in this region is the north-south boundary, or transition zone, that divides the Peninsular Ranges batholith into western and eastern regions (Jachens and Morton, 1991; Schmidt et al., 2002; Morton et al., this volume). Evidence for the transition zone comes from contrasts in lithology, major and trace elements, stable isotopes, geophysical properties, and emplacement ages (Baird and Miesch, 1984; Morton and Miller, 1987; Silver and Chappell, 1988; Kistler and Morton, 1994; Morton and Kistler, 1997; Kistler et al., 2003).

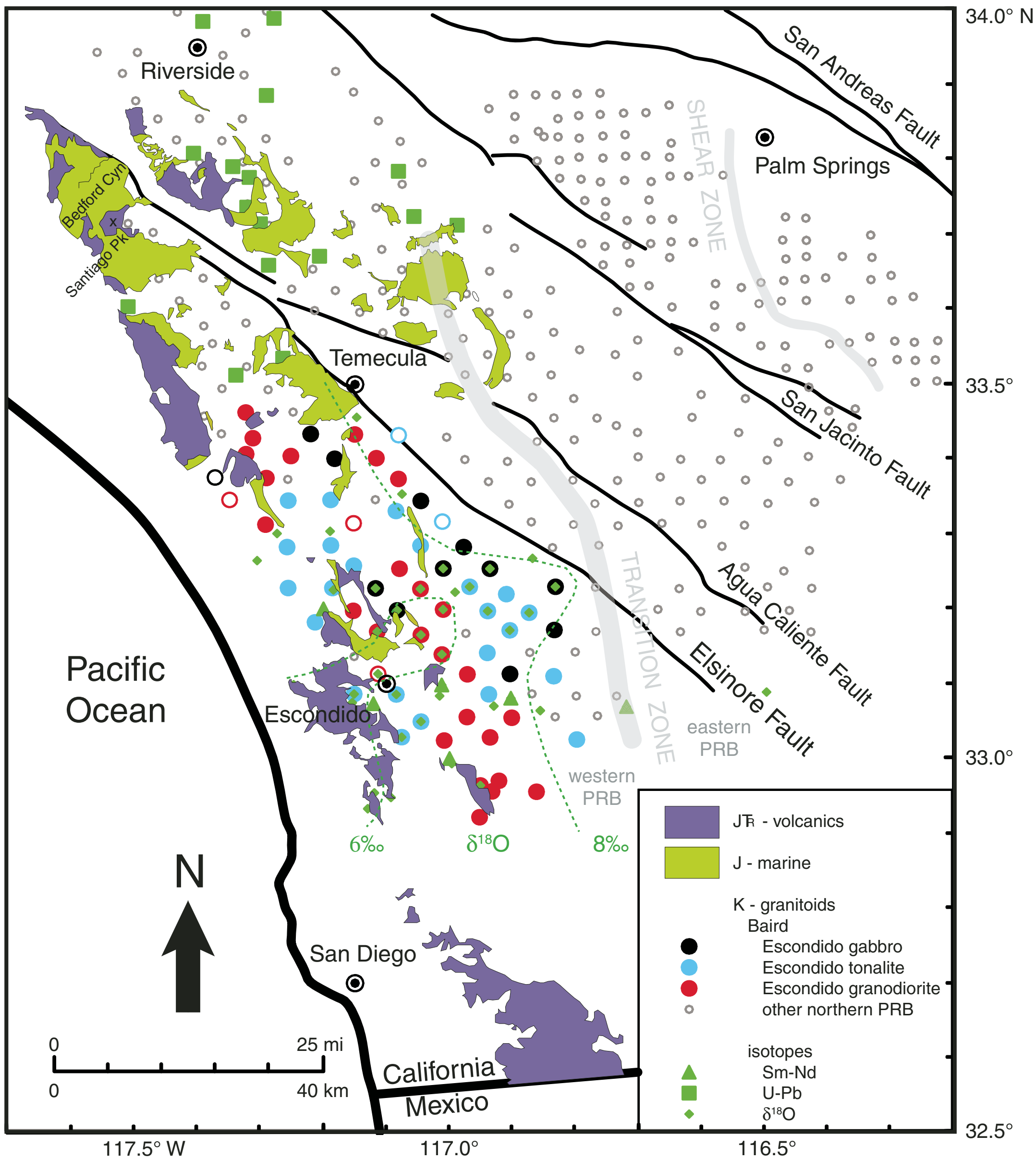

Figure 1. Map for the northern Peninsular Ranges batholith (PRB) in southern California showing major faults and the transition and shear zones. Distribution of pre-Cretaceous Santiago Peak volcanics and Bedford Canyon and French Valley marine metasediments are redrawn from Rogers (1965) and Strand (1962). Circles show the location of samples collected by Baird et al. (1974a, 1979): Black, blue, and red circles locate the Escondido samples that are the subject of this report, with atypical samples shown by open circles; open gray circles locate the remaining samples, with those northeast of the San Jacinto fault being emphasized in the text. Sample locations are also shown for published Sm-Nd (DePaolo, 1981) and U-Pb (Kistler et al., 2003) isotope data. The updated $\delta^{18}O$ contours use data from Silver et al. (1979), DePaolo (1981), and Kistler et al. (2003). Ŧ—Triassic; J—Jurassic; K—Cretaceous.

In general, plutons of the northern Peninsular Ranges batholith west of the transition zone are relatively small, have discordant contacts, and have a massive, isotropic texture that displays little evidence of strain. These plutons show evidence of widespread magmatic stoping, were passively emplaced at shallow crustal levels, and cooled rapidly at pressures of 2–3 kbar or ~10 km depth (Bern et al., 2002). Small discrete plutons indicate small magma batches, suggesting that they probably were not hot enough to melt and mix extensively with local crustal host rocks.

A past study comprehensively sampled the northern Peninsular Ranges batholith at more than 500 localities in southern California (Baird et al., 1974b, 1979; Baird and Miesch, 1984), and sampling details are given in Appendix 1. Samples in the western Peninsular Ranges batholith have low-Sr_i ratios, and 67 contiguous samples near the city of Escondido having Sr_i < 0.704 were selected for this study. They will hereafter be called the Escondido plutons. The sample locations are shown in Figure 1, and the analytical data are referenced in Table A1.

Two prebatholithic rock groups associated with the Escondido plutons will be included in this discussion. The Santiago Peak volcanics, considered to be Early Cretaceous volcanic-arc rocks (Herzig, 1991; Herzig et al., this volume), have a geochemical signature similar to the Peninsular Ranges batholith gabbros (Tanaka et al., 1984). The nearby marine Bedford Canyon Formation (Larsen, 1948; Rogers, 1965) consists of metamorphosed flysch, which is thought to have been deposited in a backarc basin environment (Criscione et al., 1978).

Sample Groups and Their Relation to Previous Work

The 67 systematically collected Escondido samples clearly constitute three groups when plotted on a histogram of SiO_2 composition (Fig. 2). The SiO_2 distribution, with distinct gaps at 54%–57% and 66.5%–68.4% SiO_2, can be fit with three Gaussian peaks. This paper will use the generic terms "gabbro," "tonalite," and "granodiorite" for the three groups.

The correspondence between the groups identified here and the plutons identified by Larsen (1948) for this area is shown in Table A1. Twelve Escondido gabbro samples have a SiO_2 content between 46.5% and 54% and correspond approximately to Larsen's San Marcos gabbro. One atypical gabbro with 46.5% SiO_2 has ultramafic characteristics and will be shown by an open circle in all plots. Twenty-five Escondido tonalite samples have a SiO_2 content between 57% and 66.5% and correspond approximately to Larsen's Bonsall and Green Valley tonalites. Two atypical tonalite samples at the high end of the range, with 66.1% and 66.5% SiO_2, have geochemical similarities to granodiorite and gabbro, respectively, and will be plotted using open circles. Thirty Escondido granodiorite samples have SiO_2 contents between 68.4% and 77.4% and correspond approximately to Larsen's Woodson Mountain and Lake Wolford granodiorites. Three somewhat atypical granodiorite samples at the low end of the range, with 68.4%, 68.7%, and 69.4% SiO_2, tend to have distinct compositions and will be plotted with open circles to set them apart. The five atypical samples fall in the 66–70% SiO_2 gap between tonalites and granodiorites.

Age Data for Sr_i Determinations

The Sr_i values were calculated for each individual sample by assuming a reasonable sample age and using

$$Sr_i = {}^{87}Sr/{}^{86}Sr|_i = {}^{87}Sr/{}^{86}Sr - {}^{87}Rb/{}^{86}Sr \times \lambda t. \quad (1)$$

For this purpose, Kistler et al. (2003) used Rb-Sr ages for Larsen's (1948) units: 105.2 ± 8.1 Ma for the Bonsall tonalite, 117 ± 14 Ma for the Green Valley tonalite, and 123.7 ± 5.6 Ma for the Woodson Mountain granodiorite. Ages for other units came from zircon ages or an assumed age of 100 Ma.

Some U-Pb data indicate variability in the age estimates. For shallow plutons of the western Peninsular Ranges batholith just north of the Escondido plutons, zircon sensitive high-resolution ion microprobe (SHRIMP) ages of 122.0 ± 0.90 Ma and 125.4 ± 1.7 Ma were obtained for Bonsall tonalite and isotope dilution–thermal ionization mass spectrometry (ID-TIMS) ages of 120.4 ± 0.45 Ma and 123.0 ± 1.1 Ma were obtained for Woodson Mountain granodiorite (Premo et al., 1998, 2002).

It is generally accepted that magmatism in the western Peninsular Ranges batholith lasted for some 20 m.y. (see, e.g., Silver and Chappell, 1988); however, different age determinations may not indicate separate magmatic events, since a deep magma chamber may have remained viable for longer than previously estimated. Whittington et al. (2009) recently determined that the thermal diffusivity at lower-crustal temperatures may be half that previously accepted, resulting in greater insulation and the possibility of longer-lived magma chambers in the lower crust.

Several references suggest a single magmatic event. Larsen (1948) indicated that the San Marcos gabbro is older than the other units, but the Bonsall and Green Valley tonalites intruded the gabbro in some places "before the latter was completely consolidated." Silver et al. (1979) obtained ages of 105–120 Ma for zircons in 21 intrusives east of San Diego and south of the Escondido plutons. They found "no clear separation of ages by lithology," but "magmas of all types were emplaced synchronously throughout a 15 m.y. interval."

To check the dependence of Sr_i on assumed age, the Rb-Sr isotope data of Kistler et al. (2003) for the Escondido pluton samples are plotted in Figure 3. Separate least-squares fits are shown as well as a single line to fit all the data. The single line yields a calculated age of 121 ± 2 Ma and an intercept of Sr_i = 0.70364. If this single age is used to calculate the Sr_i values, the values are still less than 0.704, and in most cases little changed, so the calculated Sr_i values are not critically dependent on the assumed age.

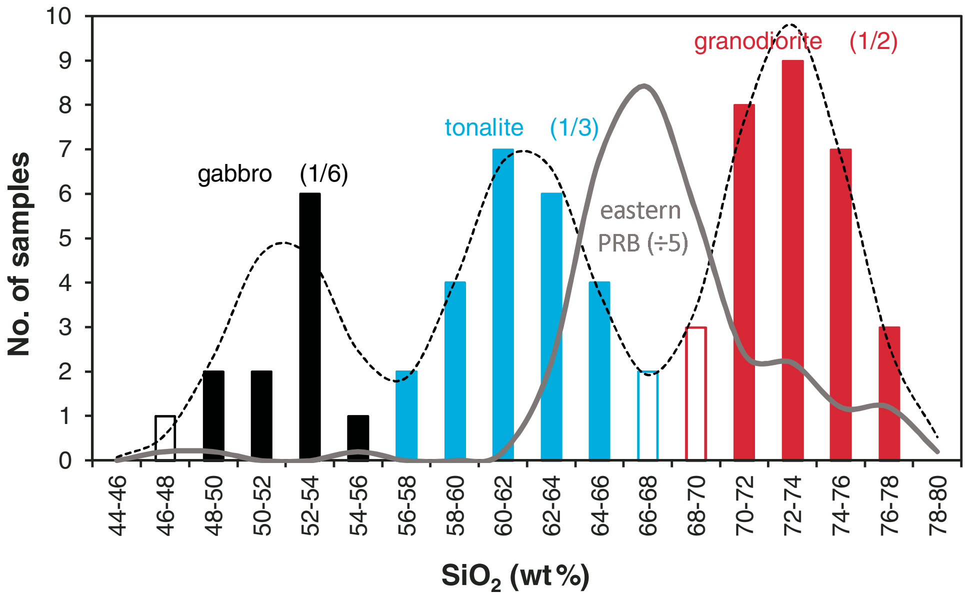

Figure 2. Histogram showing the SiO_2 distribution for the Escondido samples. The data are fit using three Gaussian peaks centered at 51.9 ± 2.4% SiO_2 for gabbro (a sixth of data), 61.9 ± 2.7% SiO_2 for tonalite (a third of data), and 72.8 ± 2.6% SiO_2 for granodiorite (a half of data). For comparison, the solid gray line represents the SiO_2 distribution for samples east of the transition zone (divided by a factor of 5). Unfilled histogram bars represent atypical data. PRB—Peninsular Ranges batholith.

MAGMATIC SOURCE REGION

The geochemistry of the Escondido plutons indicates that they formed (1) in a volcanic-arc tectonic region (2) from a tholeiitic to calc-alkaline magma source (3) by calcic to calc-alkaline differentiation (4) at a relatively shallow level (5) with no contamination from continental crust.

Volcanic-Arc Tectonic Region

Discrimination diagrams indicate that the tectonic region for the source of the Escondido granitoids was a volcanic arc, and the magma source had a composition like that of the Santiago Peak basaltic andesites and Escondido gabbros. Using Vermeesch's (2006) classification trees and diagrams, TiO_2 and Sr

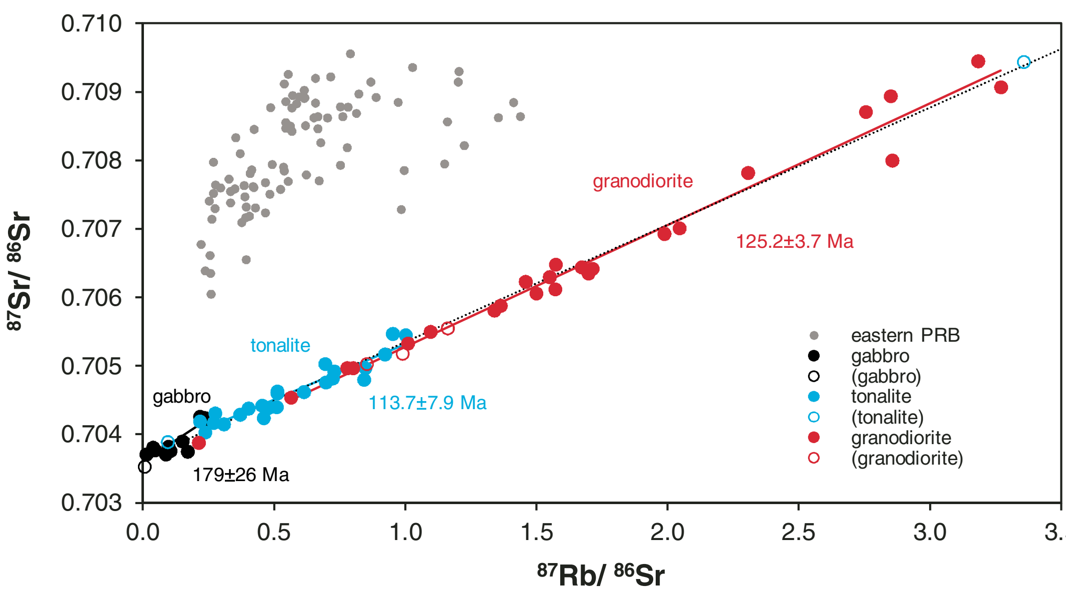

Figure 3. Rb-Sr isotope data from Kistler et al. (2003) for the Escondido plutons. The three solid lines are least-squares fits to the separate gabbro, tonalite, and granodiorite data. Using the single dotted line to fit all of the data yields an age of 121 ± 2 Ma. Gray circles representing data from the eastern Peninsular Ranges batholith (PRB) east of the San Jacinto fault contrast the scatter from crustal contamination. Note: each data point's measured $^{87}Sr/^{86}Sr$ ratio is not the same as its calculated $^{87}Sr/^{86}Sr|_i = Sr_i$ ratio, which is a smaller, y-intercept ratio based on an assumed age.

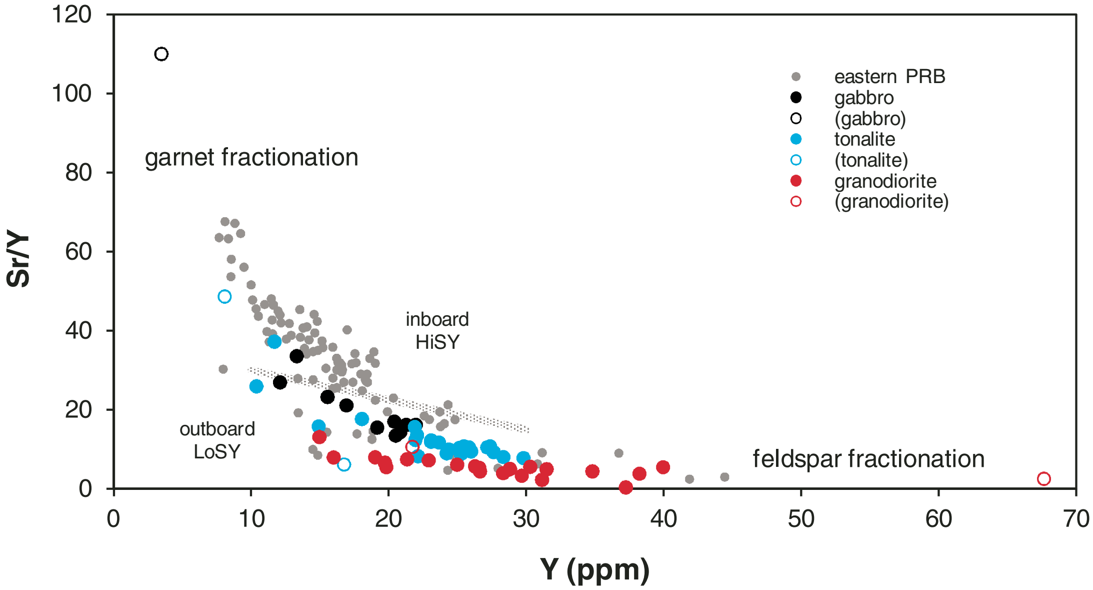

Figure 4. The Sr/Y ratio plotted against Y. The outboard low-Sr/Y Escondido samples show the effects of feldspar fractionation, whereas the inboard high-Sr/Y eastern Peninsular Ranges batholith (PRB) samples have a lower Y composition due to garnet fractionation (Tulloch and Kimbrough, 2003).

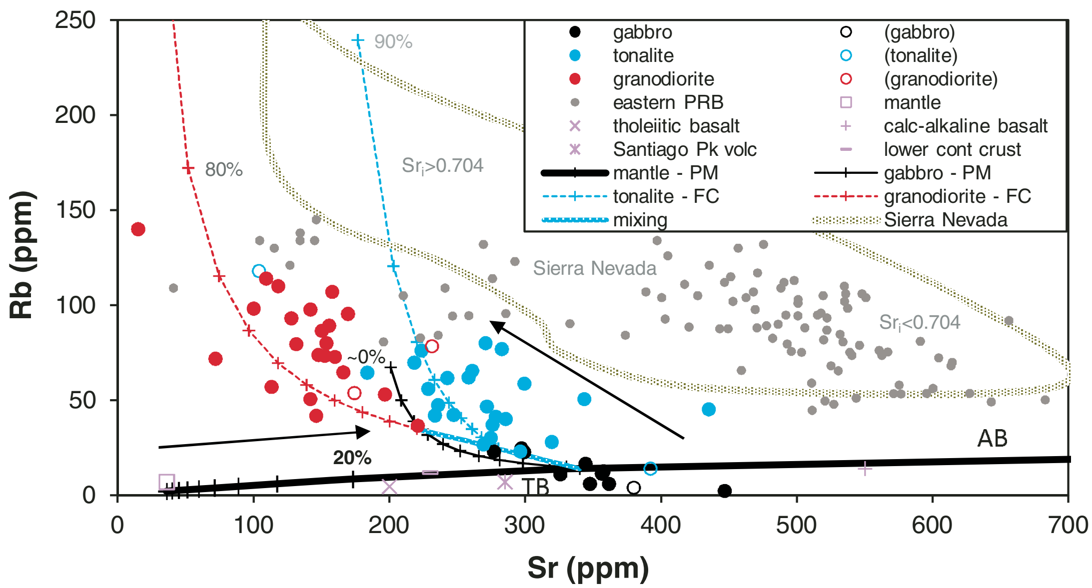

Figure 5. Partial melting (PM), magma mixing, and fractional crystallization (FC) calculations for differentiation of Rb and Sr in the Escondido plutons. For FC calculations on tonalite, $D_{Sr} = 1.2$ and $D_{Rb} = 0.01$ were used. Arrows indicate the direction of the two differentiation cycles. Tick marks represent melt fraction in 10% steps. Atypical Escondido samples are shown as open circles. According to Kistler and Peterman (1978), the Rb-Sr concentrations would indicate that the Escondido plutons differentiated from a more tholeiitic basalt (TB), whereas the eastern Peninsular Ranges batholith (PRB) and Sierra Nevada plutons differentiated from a more alkaline basalt (AB). Data sources are as follows: mantle garnet lherzolite (Grégoire et al., 2003), normal-MORB (Basaltic-Volcanism-Study-Project, 1981; Sun and McDonough, 1989), island-arc tholeiitic basalt (Hawkesworth et al., 1977; Perfit et al., 1980; Sun, 1980; Wilson, 1989), island-arc calc-alkaline basalt (Perfit et al., 1980; Sun, 1980; Wilson, 1989); Santiago Peak volcanics (Tanaka et al., 1984; Herzig, 1991) values are an average of samples with $SiO_2 < 54\%$, and lower continental crust (McLennan et al., 2006).

concentrations are found to be the best discriminators, and concentrations of TiO_2 < 1.285% and Sr > 156 ppm for the Escondido gabbros indicate an island-arc basalt composition. In Pearce's (1983) Zr/Y versus Zr plot, the Escondido gabbros and Santiago Peak basaltic andesites fall in the volcanic-arc basalt region, with some plotting as oceanic arc and some as continental arc based on a dividing line at Zr/Y = 3.

In addition to a field for arc basalts/gabbros, several bivariate plots include a field for felsic volcanic-arc rocks. Pearce et al.'s (1984) Ta versus Yb discrimination diagram places the Escondido samples within the volcanic-arc granite (VAG) field. The Sr/Y versus Y plot of Figure 4 places most of the felsic arc rocks of the Escondido plutons in the outboard low-Sr/Y field (Defant and Drummond, 1990; Tulloch and Kimbrough, 2003).

Magma Source and Differentiation Trend

The composition of the magma source for the Escondido granitoids was tholeiitic basalt, according to the Rb-Sr diagram of Figure 5. This is in contrast to the more alkaline basalt source for the eastern Peninsular Ranges and the Sierra Nevada batholiths (Kistler and Peterman, 1978). The composition corresponds to that of the Escondido gabbros and Santiago Peak basalts, which range from tholeiitic to calc-alkaline according to trace-element data on the multi-element diagram of Figure 6. Four of the gabbro samples with SiO_2 of 50% or less have a Rb composition even less than the 8 ppm average for island-arc tholeiitic basalt (Hart et al., 1970).

Differentiation of the Escondido granitoids starts with a low-K tholeiitic to calc-alkaline composition and extends into the medium-K calc-alkaline region on a standard FeO*/MgO versus SiO_2 plot (Miyashiro, 1974), the AFM (alkalis-iron-magnesium oxides) triangle, and the K_2O Harker diagram in Figure 7 (Ewart, 1982; Le Maitre, 2002). On a total-alkali-silica (Na_2O + K_2O against SiO_2) diagram, the Escondido plutons plot on the boundary between tholeiites and high-alumina basalts of Kuno (1968).

The modified alkali-lime index (Na_2O + K_2O – CaO against SiO_2) actually shows the Escondido plutons to be calcic rather than calc-alkaline, and thus from a less-mature volcanic arc (Frost and Frost, 2008). In general, the western Peninsular Ranges batholith is more calcic, and the eastern Peninsular Ranges batholith is more calc-alkaline.

Shallow Magma Source and Differentiation

Olivine crystallization for the Escondido gabbros during the earliest stages of differentiation is indicated by their range of MgO concentrations (see Fig. 8), and olivine gabbros do occur locally in the western Peninsular Ranges batholith (Larsen, 1948), including Escondido sample B477. Since olivine is the dominant fractionating mafic mineral under relatively low-pressure conditions of less than 10 kbar (Meen, 1990; Barnes et al., 2006), the olivine implies that the Escondido gabbros crystallized at shallow depths.

Garnet was not in the source for the Escondido magmas, as indicated by the gentle slope for the data in the rare earth element (REE) spidergram of Figure 9B. A steep slope on this spidergram identifies melts that have differentiated in the garnet stability zone below 10–12 kbar (Tepper et al., 1993; Moyen and Stevens, 2006). For comparison, the figure shows the steep slope for the large new REE database of eastern Peninsular Ranges batholith samples east of the San Jacinto fault. Previously, Gromet and Silver (1987) used similar data to demonstrate that the source for the western Peninsular Ranges batholith plutons was shallower than the eastern ones.

Significant amphibole differentiation occurred in the western Peninsular Ranges batholith, as indicated in Figure 10 by a decreasing Dy/Yb ratio with differentiation. This results from magmas that stall and cool in the mid- to lower crust at 8 kbar where amphibole is stable. (Davidson et al., 2007). In contrast, the Dy/Yb ratio increases with garnet differentiation in the eastern Peninsular Ranges batholith plutons.

The effects of shallow-level feldspar differentiation can be seen in plots of the alkali and alkaline earth elements. In Figure 11A, a plot of K_2O against Na_2O shows that both alkali oxides increase with SiO_2 content, but that within the granodiorite data, K_2O increases as Na_2O decreases during fractional crystallization of feldspar. In Figure 11B, the data plot of Sr against CaO shows that during feldspar fractionation in granodiorite, the Sr/CaO ratio remains constant at 0.010, as a result of the bulk distribution coefficients being approximately the same for Sr and Ca. In contrast, the range of Sr/CaO ratios for the tonalite data suggests that a different process, such as magma mixing discussed later, might be important in its formation.

The Sr/Y ratio plotted in Figure 4 summarizes the effect of garnet and plagioclase fractionation on rock geochemistry in a subduction zone. Fractionation at depth in the garnet stability zone where plagioclase is less stable leaves garnet, Y, and the HREEs (heavy rare earth elements) in the residue, and depletes the melt of Y. Fractionation at shallower levels, where plagioclase is stable and garnet is not, leaves plagioclase, Sr, and Eu in the residue, depleting the melt of Sr. The shallow-level differentiation that produced the Escondido plutons in the western Peninsular Ranges batholith yields low Sr/Y ratios, whereas the deep-level differentiation that produced the eastern Peninsular Ranges batholith yields higher Sr/Y ratios (Tulloch and Kimbrough, 2003).

No Continental Crust Contamination

Based on trace-element ratios, the Escondido plutons are relatively uncontaminated by continental crust. Trace-element ratios that have been used to identify crustal contamination include: Nb/Zr (Weaver et al., 1972; Wilson, 1989; Machida et al., 2008), Nb/Yb (Pearce, 1983; see Eby, 1990), Ta/Tb (Treuil and Varet, 1973), Ta/Yb (Barton, 1990), La/Zr (Weaver et al., 1972; Wilson, 1989), and La/Yb (Bussell, 1985). These trace-element ratios are relatively constant with differentiation for the western

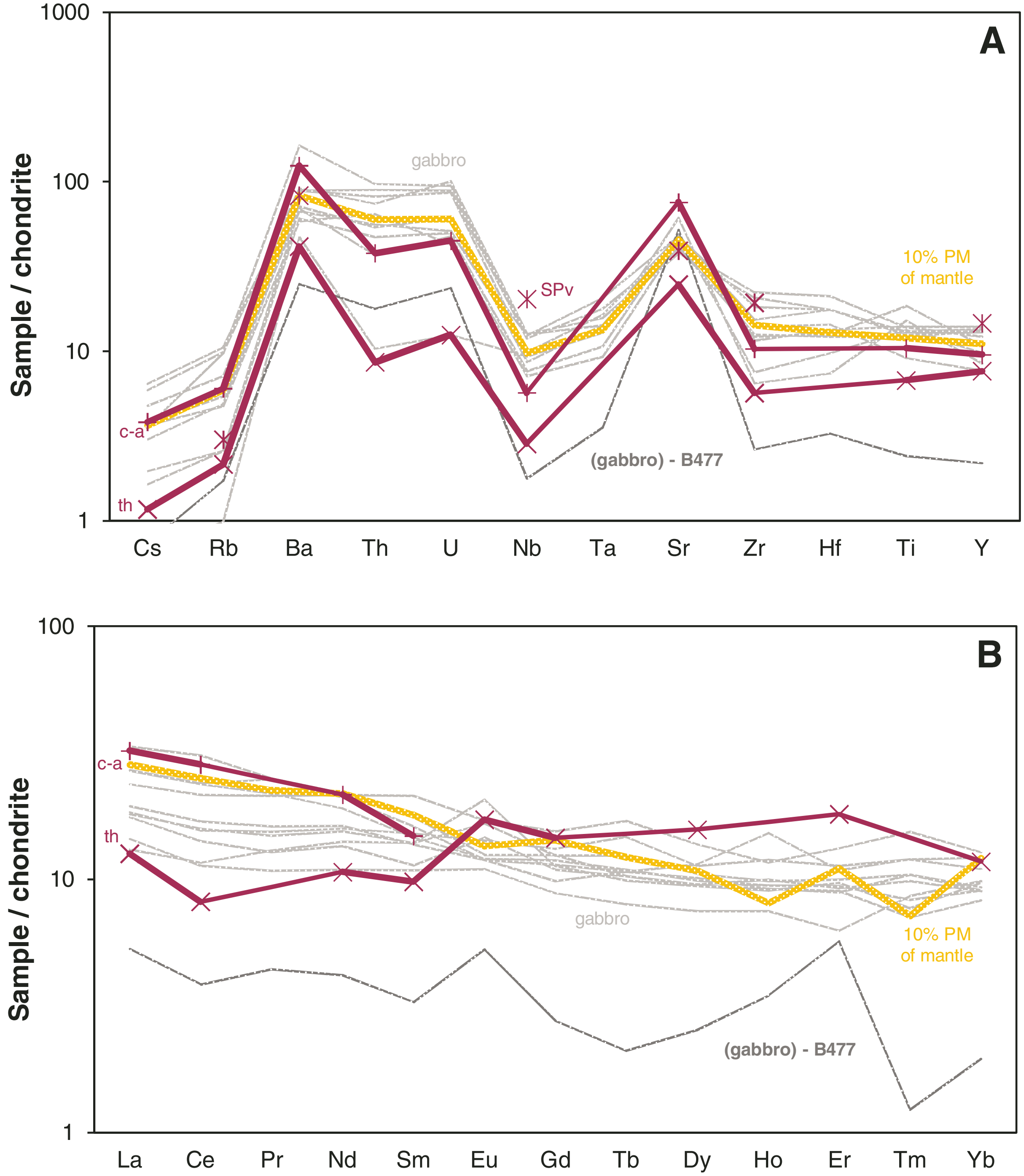

Figure 6. (A) Trace and (B) rare earth multi-element variation diagrams (spidergrams) for the Escondido gabbros and Santiago Peak volcanics (SPv) with SiO_2 less than 54%. These are compared to calc-alkaline (c-a) and tholeiitic (th) basalt values (Hawkesworth et al., 1977; Sun, 1980; Tulloch and Kimbrough, 2003), as well as to calculations for 10% partial melting (PM) of mantle. Gabbro sample B477 is atypical and may be restite from partial melting. The trace elements are normalized to Sun and McDonough (1989), and rare earth elements are normalized to Boynton (1984).

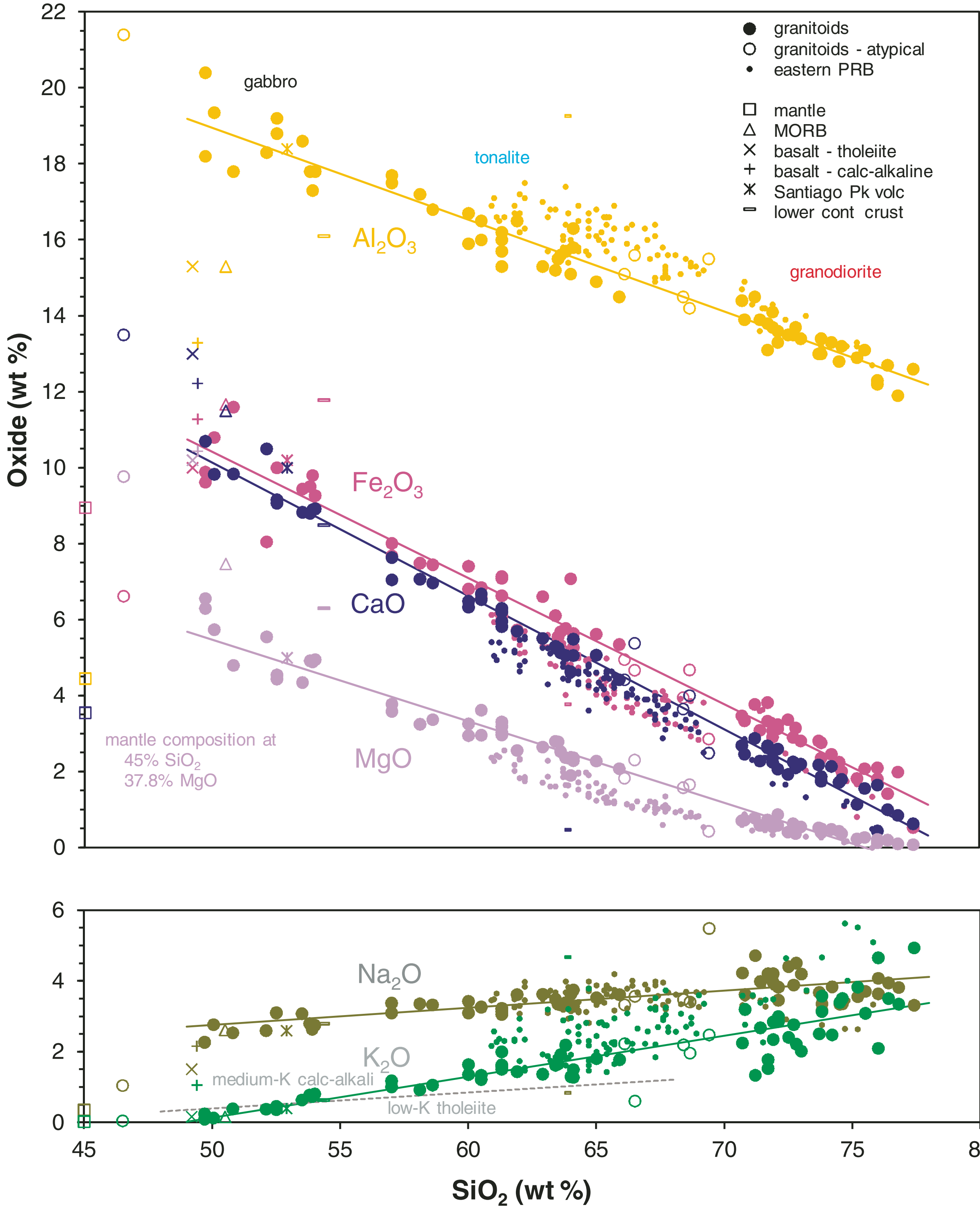

Figure 7. Harker diagram showing the major-oxide data for the Escondido samples compared to data from the eastern Peninsular Ranges batholith (PRB) and to various possible source areas. Good straight-line least-squares fits to the data provide evidence for magma mixing. Short dash symbols (-) are for the Bedford Canyon Formation (Criscione et al., 1978). MORB—mid-ocean-ridge basalt. More details are given in the Figure 5 caption.

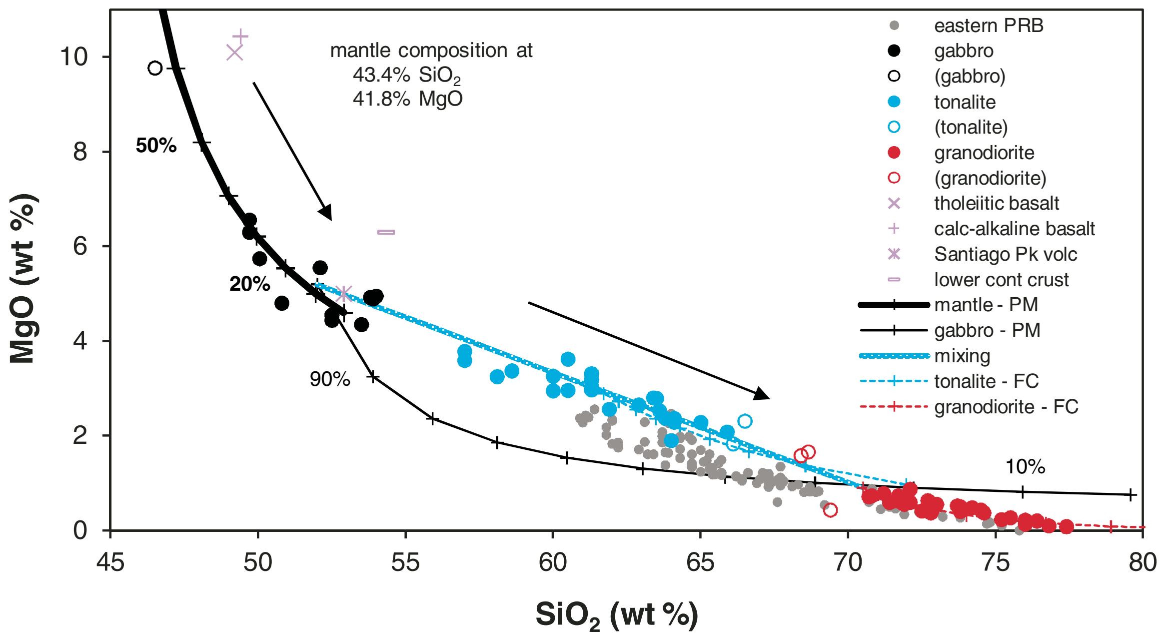

Figure 8. Partial melting (PM), magma mixing, and fractional crystallization (FC) calculations for MgO in the Escondido plutons. For FC calculations on tonalite, $D_{MgO} = 1.5$ and $D_{SiO2} = 0.93$ were used. More details are given in the caption for Figure 5. PRB—Peninsular Ranges batholith.

Peninsular Ranges batholith Escondido plutons, but they span a range of values for the eastern Peninsular Ranges batholith, where contamination from the continental crust is known to be significant (Kistler et al., 2003). Due to increasing crustal contamination, the ratios increase eastward as follows: Nb/Zr of 0.038 ± 0.018 to 0.064 ± 0.021; Nb/Yb of 1.4 ± 0.4 to 7.0 ± 2.7; Ta/Tb of 0.56 ± 0.27 to 1.5 ± 0.6; Ta/Yb of 0.15 ± 0.09 to 0.63 ± 0.26; La/Zr of 0.12 ± 0.05 to 0.19 ± 0.06; La/Yb of 4.5 ± 1.8 to 22 ± 11. The Nb/Yb ratio plotted as a function of SiO_2 in Figure 12 is the most distinctive, with an increase of less than 30% with differentiation in the western Peninsular Ranges batholith, in contrast to a factor of 5 variation with contamination in the eastern Peninsular Ranges batholith east of the San Jacinto fault.

Stable isotope ratios from the Escondido plutons for Sr and Pb (Kistler et al., 2003), for O (Silver et al., 1979; DePaolo, 1981; Kistler et al., 2003), and for Nd (DePaolo, 1981) fit within the ranges expected for arc basalts that have experienced little crustal contamination: a $^{87}Sr/^{86}Sr$ ratio of 0.703–0.704, a $^{206}Pb/^{204}Pb$ ratio of 18.4–19.0, a $^{207}Pb/^{204}Pb$ ratio of 15.5–15.7, a $^{208}Pb/^{204}Pb$ ratio of 38.0–38.7, $\delta^{18}O$ of 5‰–8‰, and a $^{143}Nd/^{144}Nd$ ratio of 0.5129–0.5131 (Arculus and Powell, 1986; White and Dupré, 1986; Wilson, 1989).

The $\delta^{18}O$ contour lines in Figure 1 show that the Escondido plutons have values of less than 8‰, suggesting a primitive source not from continental crust (Magaritz et al., 1978; James, 1981; Wilson, 1989). According to Taylor and Silver (1978), the plutons of the western Peninsular Ranges batholith have undergone little contamination by the local metasedimentary rocks, such as the Bedford Canyon Formation, which have $\delta^{18}O$ values from 11‰ to 20‰. Usually, $\delta^{18}O$ values for igneous rocks increase with increasing SiO_2 concentration (Faure, 1986), but the Peninsular Ranges batholith variations are mainly geographic rather than dependent on rock type.

Additional insight on the low-Sr_i values for the Escondido plutons comes from a comparison with data from further north and east in the Peninsular Ranges batholith. The locations for the Escondido samples shown in Figure 1 have few associated marine sedimentary rocks available for contamination, in contrast to the remainder of the Peninsular Ranges batholith to the north and east, which are associated with a significant amount of sedimentary rock. The Escondido Rb-Sr isotope data plotted in Figure 3 fall on a straight line ($R^2 = 0.99$), suggesting an uncontaminated source, in contrast to the Rb-Sr isotope data for plutons in the eastern Peninsular Ranges batholith, which display a great deal of scatter ($R^2 = 0.6$), suggesting significant crustal contamination.

CALCULATIONS FOR A TWO-CYCLE MODEL

Significance of the Low-Sr_i Escondido Plutons

Formation of continental crust is thought to occur primarily at active continental margins as a result of vertical accretion of volcanic and plutonic material and lateral accretion of oceanic arcs to continental cratons (Weaver and Tarney, 1982; Leat and Larter, 2003; Brown and Rushmer, 2006), but the process that yields continental crust with an average composition of andesite is not well understood (see, e.g., Kodaira et al., 2007). One

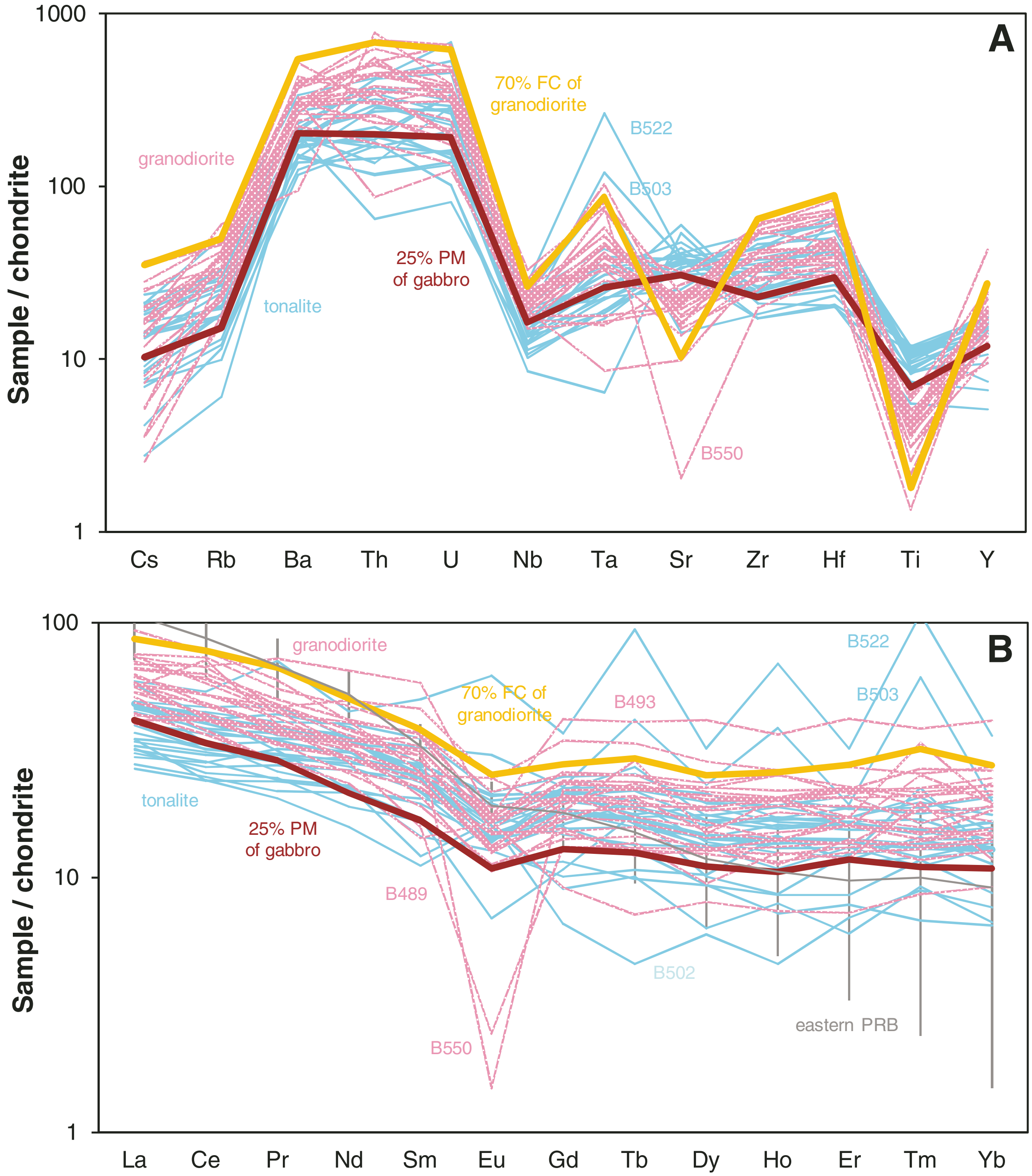

Figure 9. (A) Trace and (B) rare earth multi-element variation diagrams for the Escondido tonalites and granodiorites. These are compared to calculations for 25% partial melting (PM) of a gabbro/amphibolite source and 70% fractional crystallization (FC) of the resulting granodiorite magma, as well as to the mean and standard deviation for eastern Peninsular Ranges batholith (PRB) data. Unique samples are labeled: B493, B489, and B550 samples were strongly affected by plagioclase differentiation; B503 and B522 probably had large uncertainties from measuring odd-atomic-numbered elements with low concentrations; B502 is one of the atypical tonalites. The trace elements are normalized to Sun and McDonough (1989), and rare earth elements are normalized to Boynton (1984).

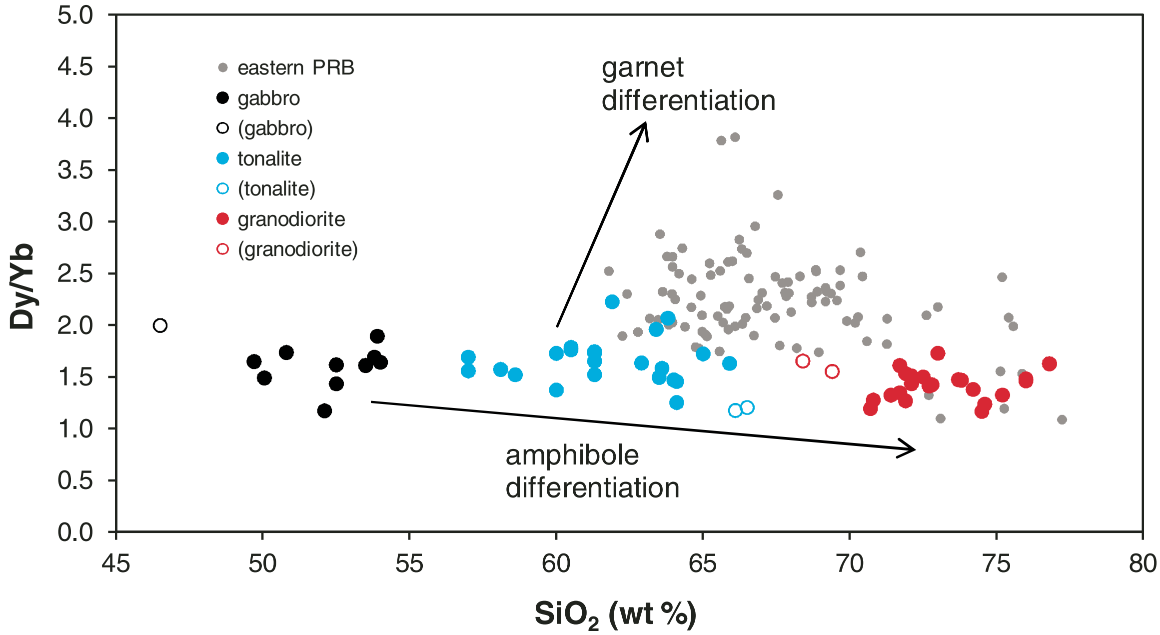

Figure 10. As with most arc volcanoes, the western Peninsular Ranges batholith (PRB) Escondido plutons exhibit trends of decreasing Dy/Yb with differentiation. This is consistent with significant amphibole, but not garnet, differentiation (Davidson et al., 2007). Atypical Escondido samples are shown as open circles.

of the suggested models involves a two-cycle process in which (1) basaltic magma from the mantle forms a mafic crust, which (2) melts and differentiates, yielding felsic magmas that mix with mafic magmas (Taylor, 1967; Pearcy et al., 1990; Rudnick, 1995; Kelemen et al., 2003). In the two-cycle process, remelting and mixing in the lower crust and delamination of cumulates and restites result in the andesitic continental crust observed today (Tatsumi and Kogiso, 2003; Annen et al., 2006; Davidson and Arculus, 2006).

Igneous rocks, especially the extensive list of Faure (2001), that are formed by one, two, or more cycles, are categorized in Table 1 based on the number of cycles they have experienced and their resulting Sr_i values and SiO_2 compositions. One cycle of mantle partial melting, magma transport and emplacement, and fractional crystallization yields mafic crustal rocks with low-Sr_i and low-SiO_2 composition, e.g., the Peninsular Ranges "batholith-associated" Santiago Peak volcanics. A second cycle of partial melting of mafic crust and fractional crystallization yields felsic crustal rocks with low-Sr_i and high-SiO_2 composition, if no contamination from continental crust occurs, e.g., the Escondido plutons. A third (or higher) cycle occurs if continental crust is involved in the partial melting and fractional crystallization, and the result is continental crust with high-Sr_i and high-SiO_2 composition, e.g., the eastern Peninsular Ranges batholith.

The three cycles can be conveniently understood in terms of the changes in Sr_i and SiO_2, which are illustrated in Figure 13. This is a standard textbook figure (see Faure and Mensing, 2005), but with details and a description unique to the situation described here. The generic data in this figure are representative of Kistler et al.'s (2003) data from the northern Peninsular Ranges batholith. The isotope ratios change due to three processes. (a) Diffusion: Melting and magma mixing yield homogeneous $^{87}Sr/^{86}Sr$ ratios throughout the magma and an increase in average Sr_i. (b) Differentiation: Partial melting and fractional crystallization increase the $^{87}Rb/^{86}Sr$ ratios (and SiO_2 composition) due to different mineral partitioning of Rb and Sr, but the $^{87}Sr/^{86}Sr$ ratios remain uniform and unaffected by chemical partitioning. (c) Decay: After crystallization, the ^{87}Rb composition decreases, and the ^{87}Sr composition (and corresponding $^{87}Sr/^{86}Sr$ ratio) increases, causing the horizontal line to rotate counterclockwise around the fixed initial $^{87}Sr/^{86}Sr = Sr_i$ value on the *y*-intercept.

The significance of the Escondido plutons lies in their low-Sr_i and high-SiO_2 composition, which recently formed by this two-cycle process. (1) The uniformly low-Sr_i values for the Escondido plutons indicate that *no more than* two differentiation cycles occurred, so magma source, initial composition, and differentiation processes are simpler to model in calculations. A similar two-cycle process of continental crust formation occurred in the Precambrian, but the results are often obscured by more recent geological events. (2) The full range of SiO_2 compositions for the Escondido plutons indicates that *no less than* two cycles occurred, so a complete set of magma differentiation calculations can quantify the geochemical processes for forming continental crust of intermediate composition. A similar range of SiO_2 compositions is ubiquitous in Phanerozoic crust, but it is usually complicated by a third cycle (or more) of contamination by preexisting continental crust.

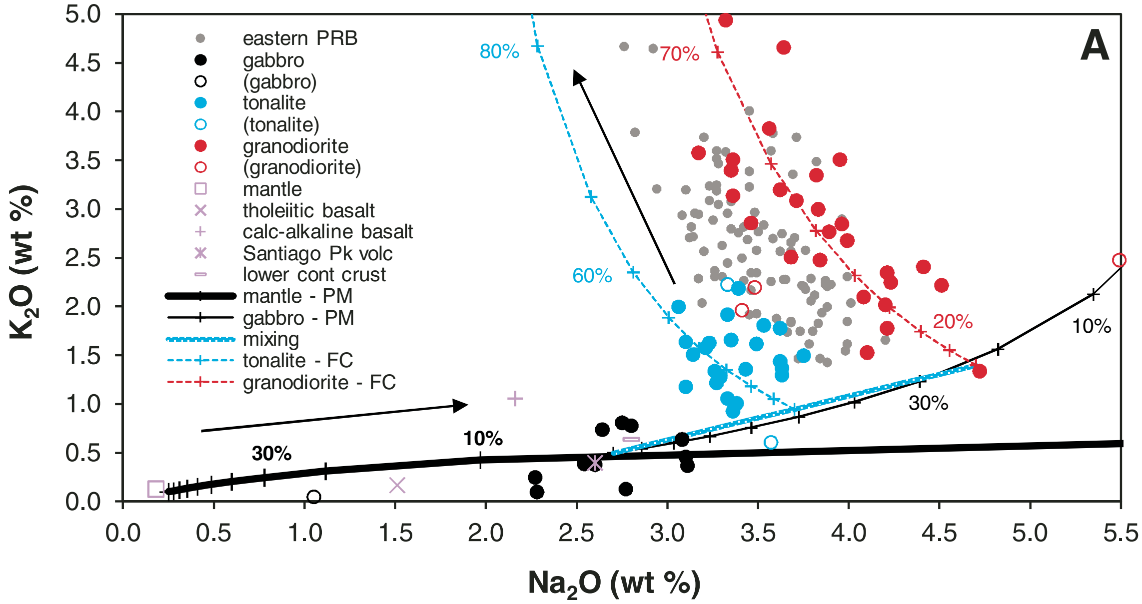

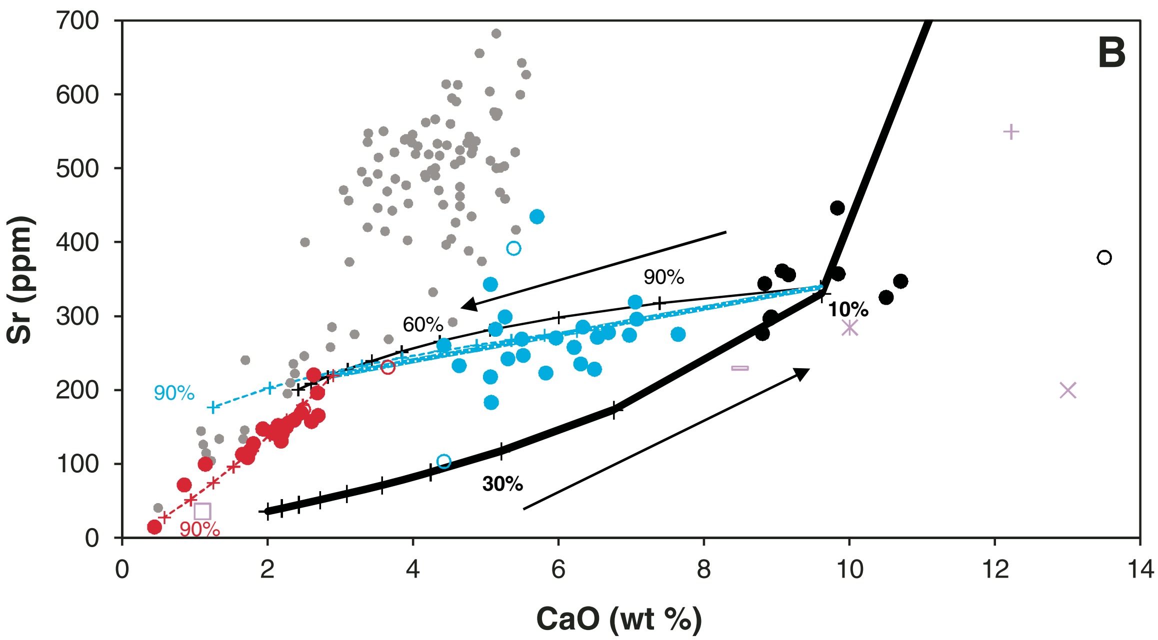

Figure 11. (A) Partial melting (PM), magma mixing, and fractional crystallization (FC) calculations for the alkali oxides in the Escondido plutons. For FC calculations on tonalite, $D_{K2O} = 0.01$ and $D_{Na2O} = 1.3$ were used. More details are given in the caption for Figure 5. The Na_2O composition increases during partial melting of the gabbro but decreases during fractional crystallization of the granodiorite melt. (B) This plot shows decreasing Sr and CaO concentrations as felsic differentiation proceeds. The Sr/CaO ratio is changed by mixing, but it remains constant with fractionation. For FC calculations on tonalite, $D_{Sr} = 1.2$ and $D_{CaO} = 1.7$ were used. PRB—Peninsular Ranges batholith.

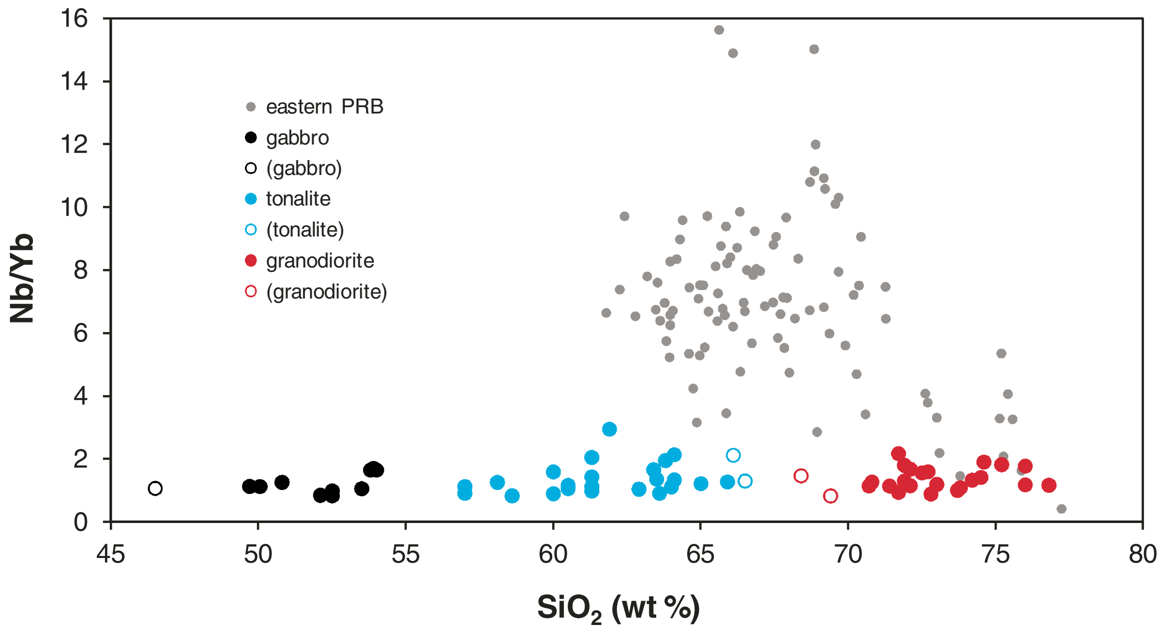

Figure 12. The Nb/Yb ratio as a function of SiO_2 for the Escondido samples compared to samples contaminated by continental crust in the eastern Peninsular Ranges batholith (PRB). The Escondido samples have a constant Nb/Yb ratio of 1.4 ± 0.4 independent of fractionation. Atypical Escondido samples are shown as open circles.

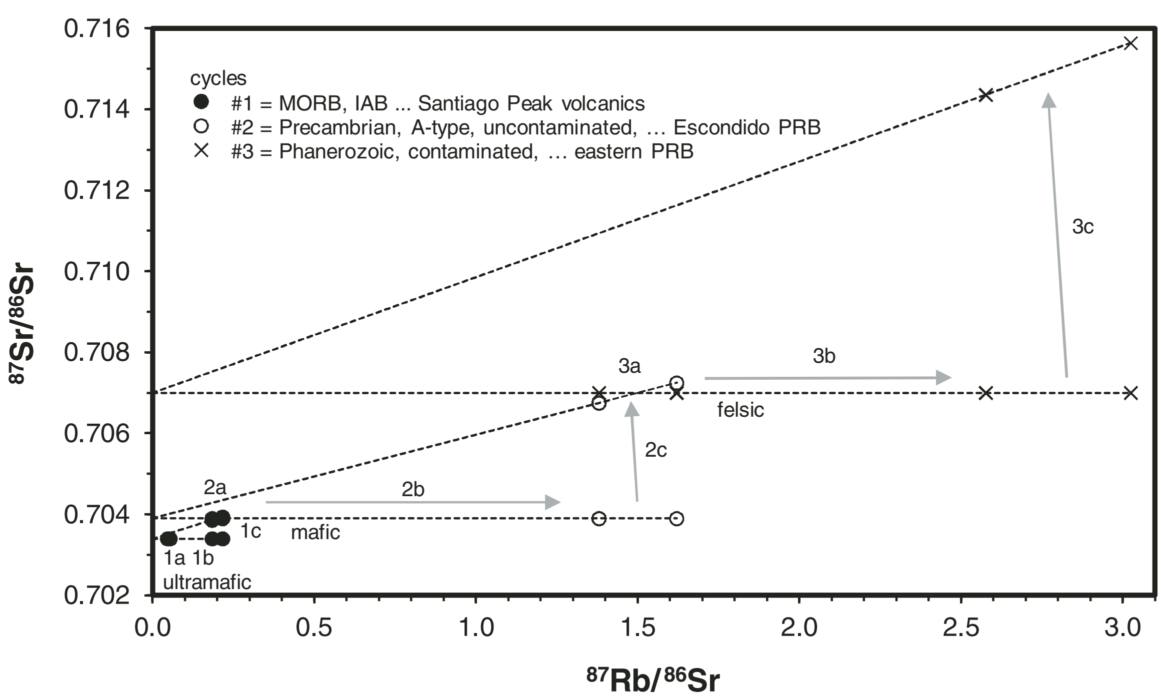

Figure 13. The evolution of Sr and Rb isotopes with time. The Sr_i (*y*-intercept) ratio, the Rb concentration, and the $^{87}Sr/^{86}Sr$ ratio begin with low values in the mantle and increase through several differentiation cycles, as explained in the text. PRB—Peninsular Ranges batholith; MORB—mid-ocean-ridge basalt; IAB—island-arc basalt.

Calculations and Conditions from the Literature

Melting and crystallization calculations have clarified the role of each process in forming the Klamath Mountains province (Barnes et al., 1986; Snoke and Barnes, 2006), the Archean tonalite-trondhjemite-granodiorites (TTGs) in Finland (Martin, 1987), adakites in Panama (Defant et al., 1991a), the Quottoon igneous complex in British Columbia (Thomas and Sinha, 1999), the Absaroka volcanic province in Wyoming (Feeley et al., 2002), plutons of central Idaho (Fleck and Criss, 1985), the Talkeetna arc in Alaska (Greene et al., 2006), and a bimodal plutonic complex in Turkey (Dokuz et al., 2006). This study applies these calculations to the Peninsular Ranges batholith.

The usual model for Phanerozoic formation and differentiation of the crust (Rudnick, 1995; Davidson and Arculus, 2006; Hawkesworth and Kemp, 2006) has been suggested for the Peninsular Ranges batholith (Gromet and Silver, 1987; Silver and Chappell, 1988) and will be used here for our Microsoft Excel calculations. Such calculations would most simply be for a single pluton, but we have already noted that the Escondido area plutons may all represent a single magmatic event. In this case, we do first-cycle calculations for formation of the gabbros, second-cycle calculations for the granodiorites, and magma mixing calculations for the tonalites.

In the first cycle, reasonable mantle conditions of 1200–1300 °C and 20–30 kbar produce a hydrous basalt from 5% to 15% partial melting (Pearce and Parkinson, 1993; Grove et al., 2003) that then forms the volcanic arc and intrudes and underplates the lower crust.

The second cycle results from heating due to intrusion of additional mantle melt (Huppert and Sparks, 1988; Bergantz, 1989; Annen and Sparks, 2002). Reasonable lower-crust conditions of 900–1000 °C at up to 10 kbar pressure result in 20%–40% dehydration partial melting of amphibolite (Gromet and Silver, 1987; Tepper et al., 1993; Petford and Gallagher, 2001; Sisson et al., 2005). The melt with roughly 3 wt% H_2O is oxidizing, and f_{O_2} spans the range from just under the QFM (quartz-fayalite-magnetite) buffer to slightly more oxidizing than the NNO (nickel-nickel oxide) buffer (Ague and Brimhall, 1988). The final crystallization occurs in tabular-shaped plutons (Petford et al., 2000; Cruden, 2006) at 5–10 km depth (Krummenacher et al., 1975), with fractional crystallization continuing in a convecting magma until 60%–70% of the magma has solidified (Vigneresse and Tikoff, 1999).

First-Cycle Calculations for the Mantle

For the first differentiation cycle, partial melting calculations for the mantle used the simple batch melting equation where C_0 is the initial elemental concentration before melting and D is the bulk distribution coefficient. The value of C_0 for each element was taken from a combination of garnet lherzolite (Grégoire et al., 2003) and spinel lherzolite (Maaløe and Aoki, 1977). To determine D, initial values based on mineral composition were varied to yield the average Escondido gabbro composition with up to 10% partial melting of the mantle. The mantle compositions C_0 are listed in Tables 2 and 3, the mineral percentages are in Table 4, and the bulk distribution coefficients D are in Table 5. Plots of these calculations are included in Figures 5, 8, 11, 14, and 15. The results of 10% partial melt calculations are shown in the Figure 6 multi-element diagrams for the trace and rare earth elements.

For comparison with this standard partial melting equation, we used equations and parameters from Williams and Gill (1989) and Pearce and Parkinson (1993). Based on calculations for the elements Nb and Yb, the Escondido gabbros would have formed from ~10% partial melting of the fertile mid-ocean-ridge basalt (MORB) mantle (FMM) as defined by Pearce and Parkinson (1993). Similar calculations for Zr, Y, Sc, V, Cr, Co, MnO, MgO, TiO_2, Fe_2O_3, CaO, and Al_2O_3 gave a range of results mostly

TABLE 2. MAJOR-ELEMENT CONCENTRATIONS

	SiO_2	Al_2O_3	CaO	Na_2O	K_2O	Fe_2O_3*	MgO	TiO_2	P_2O_5	MnO
Calculation parameters for partial melting, fractional crystallization, and mass balance calculations										
Mantle										
C_0	44	2.5	2	0.25	0.1	9	41	0.13	0.03	0.13
Restite	43.2	0.9	1.2	0.01	0.06	8.9	44	0.04	0.02	0.127
Harzburgite†	44.5	1.7	1.4	0.1	N.D.	10.67	42.6	0.04	N.D.	N.D.
Gabbro										
C_0	51.9	18.5	9.6	2.7	0.5	9.8	5.2	1	0.15	0.17
Restite	45.8	19.8	11.8	2.0	0.2	11.8	6.6	1.2	0.153	0.2
Pyroxenite§	45.17	15.11	12.7	1.39	0.41	15.06	9.81	0.4	0.11	0.3
B477	46.5	21.4	13.5	1.05	0.05	6.62	9.77	0.18	<0.05	0.11
Green Acres	42.9	16.2	10.4	0.66	0.04	9.69	19.8	0.12	<0.05	0.12
Granodiorite										
C_0	70.5	14.5	2.9	4.7	1.4	3.8	0.9	0.5	0.14	0.09
Cumulate	67.5	15.6	3.9	5.5	0.01	5	1.3	0.7	0.18	0.12
B502	66.5	15.6	5.38	3.57	0.61	4.67	2.31	0.41	0.11	0.08

Note: All concentrations are in units of wt%. N.D.—not determined.
*Total iron-oxide content.
†Harzburgite (Brown and Mussett, 1993).
§Low-MgO garnet pyroxenite (Lee et al., 2006).

TABLE 3. TRACE-ELEMENT CONCENTRATIONS

	Mantle	Gabbro	Granodiorite
The C_0 fitting parameters for partial melting and fractional crystallization calculations as described in the text:			
Cs	0.1	0.7	2
Ba	47	195	500
Rb	2	14	35
Sr	36	340	220
Th	0.3	1.8	6
U	0.07	0.5	1.5
Nb	1	2.5	4
Ta	0.07	0.2	0.37
Zr	9	55	90
Hf	0.2	1.5	3.2
Y	3	18	18.5
La	2.5	6.6	13
Ce	5	15	27
Pr	0.6	2.2	3.5
Nd	2.4	10	13
Sm	0.4	2.9	3.2
Eu	0.1	1.1	0.8
Gd	0.4	3.1	3.5
Tb	0.05	0.55	0.6
Dy	0.3	3.3	3.5
Ho	0.05	0.7	0.8
Er	0.2	2.1	2.5
Tm	0.02	0.33	0.35
Yb	0.3	2.1	2.2
Sc	12	35	16
V	50	230	60
Cr	2400	69	30
Co	100	33	8

Note: All concentrations are in units of ppm.

between 10% and 20% partial melting. This is similar to Dokuz et al.'s (2006) estimates of 15%–20% partial melting of lherzolite mantle to yield gabbro in an intrusive complex in Turkey.

Second-Cycle Calculations for the Crust

A second differentiation cycle in the crust was analyzed using the batch melting equation and the Rayleigh fractionation equation. Allègre and Minster (1978) have discussed the use of such equations for trace elements in quantitatively modeling magmatic processes. The C_0 and D values for use in the equations are determined in four steps that partially follow those used to analyze Archean TTG plutons (Martin, 1987; Stevens and Moyen, 2007).

1. A least-squares regression line was used to fit the *major-oxide data* in the Harker diagrams of Figure 7 (see, e.g., Reid et al., 1983; Frost and Mahood, 1987; Drummond et al., 1988). The R^2 values listed in Table 5 show the excellent linear correlation for most major oxides.

2. The *mineral percentages* in each pluton type were initially taken from Larsen's (1948) modal averages. The averaged oxides of step one were then used to calculate CIPW norms. The mode and norm were then combined to make a final best estimate of mineral percentages. All three sets of values are listed in Table 4.

Note that the oxide data include only Fe_2O_3 total, whereas the norm calculations require both Fe_2O_3 and FeO, so the Fe_2O_3/FeO ratios were estimated. From Larsen's (1948) data for this area, a ratio of 0.3 can be estimated for the gabbros, 0.4 for the tonalites, and 0.5 for the granodiorites. Using the total-alkali-silica diagram for volcanic rocks, Middlemost (1989) suggested a ratio of 0.2 for basalt, 0.35 for andesite, 0.4 for dacite, and 0.5 for

TABLE 4. MINERAL PERCENTAGES

	Olivine	Opx	Cpx	Garnet	Spinel
Mantle—mode					
Percent used	63	25	6	5	1

	Ca-Plag	Na-Plag	Ortho	Quartz	Amph	Biotite	Cpx	Opx	Apt	Mag	Ilm
Gabbro											
[Green Acres]	45	forsterite = 36			2		11	3	spinel = 2.5, iddingsite = 0.5		
Mode*		42	27		2	24	2	4	6		1
CIPW norm†	38.3	21.8	2.5	3.0			8.0	20.9	0.33	2.9	1.8
Percent used	35	23		3	19	1	6	10	0.35	1	1.6
Tonalite											
Mode*		26	25		18	13	18				
CIPW norm†	24.6	28.3	8.7	17.5			3.4	11.9	0.35	2.6	1.4
Percent used	24	27	1	20.8	10	10	1	3	0.38	1.3	1.5
Granodiorite											
Mode*		10	31	20	33	1	5				
CIPW norm†	24.6	28.3	8.7	17.5			3.4	11.9	0.35	2.6	1.4
Percent used	9.6	33	16.7	34.3	0.5	1.9		2	0.2	1.3	0.5

Note: The mineral percentages used to estimate bulk distribution coefficients are a best estimate from a combination of norm and mode. Ca-Plag—calcium plagioclase; Na-Plag—sodium plagioclase; Ortho—orthoclase; Amph—amphibole; Cpx—clinopyroxene; Opx—orthopyroxene; Apt—apatite; Mag—magnetite; Ilm—ilmenite.

*The average mode for each pluton type is determined from Larsen's (1948) samples, with the plagioclase split between Ca and Na based on anorthite percentage.

†The CIPW norms are calculated from average oxide values for the Escondido data.

TABLE 5. BULK DISTRIBUTION COEFFICIENTS

	Mantle PM	Gabbro PM	Granodiorite FC	R^{2}*
Major and minor elements				
SiO_2	0.83	0.65	0.93	N.A.
Al_2O_3	0.05	1.36	1.15	0.95†
CaO	0.12	4	1.7	0.98†
Na_2O	0.03	0.45	1.3	0.53
K_2O	0.15	0.15	0.01	0.78
Fe_2O_3*	0.9	3	1.7	0.92†
MgO	9	7	2.5	0.93†
TiO_2	0.05	2.3	2.1	0.73†
P_2O_5	0.13	1.1	1.8	0.30†
MnO	0.75	2.2	2.0	0.87†
Large ion lithophile mobile and high field strength immobile incompatible elements	0.9	3	1.7	0.92
Cs	0.05	0.15	0.01	0.23
Ba	0.15	0.2	0.2	0.74
Rb	0.05	0.2	0.01	0.61
Sr	0.01	1.7	1.9	0.73†
Th	0.08	0.08	0.01	0.54
U	0.05	0.1	0.01	0.35
Nb	0.35	0.5	0.6	0.50
Ta	0.3	0.4	0.01	0.05
Zr	0.07	0.5	0.15	0.41
Hf	0.05	0.3	0.1	0.38
Y	0.08	0.95	0.3	0.19
Rare earth incompatible elements (REE)				
La	0.3	0.35	0.4	0.71
Ce	0.25	0.4	0.3	0.65
Pr	0.2	0.5	0.3	0.41
Nd	0.15	0.7	0.3	0.36
Sm	0.05	0.85	0.3	0.21
Eu	0.03	1.5	0.3	0.01†
Gd	0.04	0.9	0.4	0.15
Tb	0.01	0.9	0.3	0.03
Dy	0.01	0.9	0.3	0.15
Ho	0.01	0.9	0.3	0.05
Er	0.01	0.8	0.3	0.20
Tm	0.01	0.9	0.1	0.02
Yb	0.05	0.9	0.2	0.23
Compatible elements				
Sc	0.3	2.6	2.5	0.80†
V	0.15	5	3.5	0.74†
Cr	38	2.7	2.0	0.33†
Co	3.3	5	2.5	0.94†

Note: These coefficients *D* were used in the partial melting (PM) and fractional crystallization (FC) calculations.

*The correlation coefficients for all the elements show how similar the differentiation of each is to that of SiO_2. For the major elements, it shows the strong linearity that implies magma mixing.

†Negative correlation.

rhyolite. These two estimates were combined, and the unrealistic discontinuity in ratio at field boundaries was removed by using

$$Fe_2O_3/FeO = 0.011 \times SiO_2\% - 0.31 \tag{2}$$

to estimate the iron-oxide ratio.

3. All the *initial element concentrations,* C_0, were determined by starting with the major-element oxides from the first step. The resulting C_0 values for partial melting were the average of the Escondido gabbro data (e.g., 51.9% SiO_2), and those for fractional crystallization were the least-differentiated granodiorite data (e.g., 70.5% SiO_2). These values are listed in Tables 2 and 3.

4. Bulk *distribution coefficients* for all elements were calculated using the mineral distribution coefficients of Rollinson (1993) and the mineral percentages from the second step. These coefficients were used in the initial fit to the data and then adjusted along with the initial element concentrations until a final best fit was obtained. The data fitting was done on bivariate diagrams with each of the elements plotted against SiO_2 and/or Co. The resulting bulk distribution coefficients are listed in Table 5. This table also uses R^2 to show how similar the differentiation of each element is to that of SiO_2.

The bulk distribution coefficient is defined for trace elements, but it has also been used occasionally for the major elements. For SiO_2, Kistler et al. (1986) used an effective partition coefficient

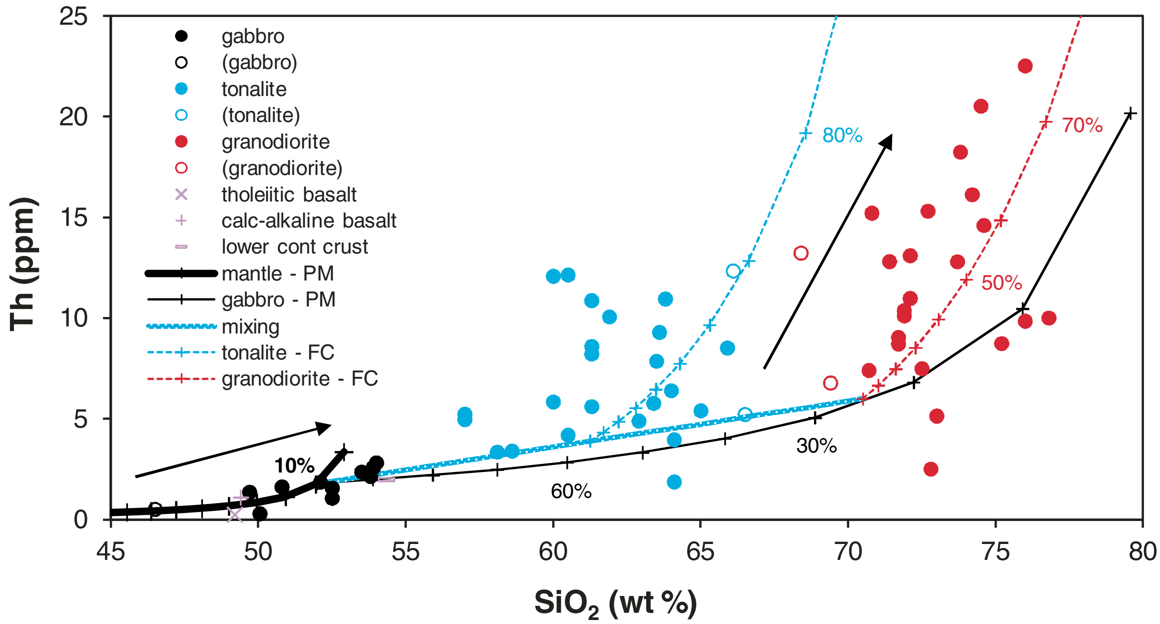

Figure 14. Partial melting (PM), magma mixing, and fractional crystallization (FC) calculations for an incompatible trace element in the Escondido plutons. For FC calculations on tonalite, $D_{Th} = 0.01$ and $D_{SiO2} = 0.93$ were used. More details are given in the caption for Figure 5.

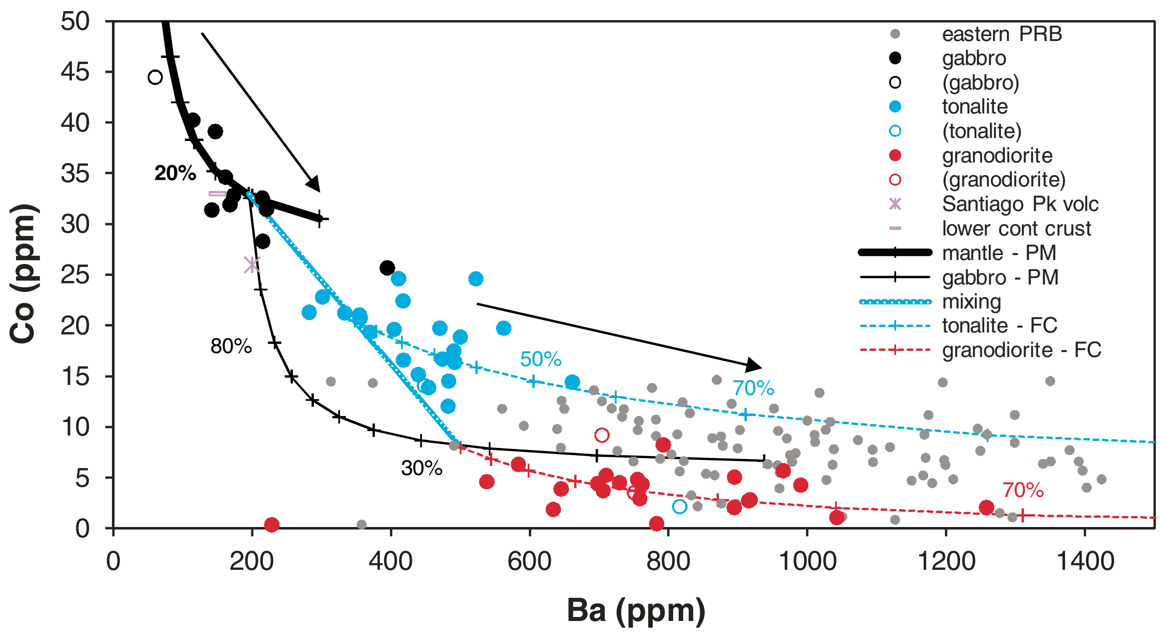

Figure 15. Partial melting (PM), magma mixing, and fractional crystallization (FC) calculations for a compatible against an incompatible trace element in the Escondido plutons. For FC calculations on tonalite, $D_{Co} = 1.5$ and $D_{Ba} = 0.2$ were used. The mantle composition is off the diagram at 105 ppm Co and 6.6 ppm Ba. More details are given in the caption for Figure 5. PRB—Peninsular Ranges batholith.

of 0.8, and Wall et al. (1987) estimated a range from 0.75 to 0.9. Dokuz et al. (2006) used effective coefficients for Na_2O, K_2O, TiO_2, and P_2O_5. The calculations done here use an effective bulk distribution coefficient for all of the major elements.

Results

A sample Harker plot with calculated curves is shown in Figure 8 for a compatible major oxide (MgO). It illustrates the two differentiation cycles with calculation curves and arrows: (1) Mantle peridotite partially melts to produce tholeiitic basalt and gabbro; (2) lower-crustal gabbro/amphibolite partially melts to produce a granodiorite magma that mixes (to be discussed in a later section) with a basaltic magma to yield an intermediate composition; the tonalite and granodiorite magmas subsequently fractionally crystallize. Additional calculated differentiation curves are shown on the bivariate plots of Figures 5, 11, 14, and 15—a pair (Rb vs. Sr) already used to determine source, two major alkali oxides (K_2O vs. Na_2O), two alkaline earths (Sr vs. CaO), an incompatible trace element (Th) versus SiO_2, and a representative compatible-incompatible pair (Co vs. Ba).

For Figures 5, 8, 11, 14, and 15, the mantle partial melting curve uses up to a 10% mantle melt to yield a composition equivalent to the Escondido gabbro/basalt. The curve for the ensuing fractional crystallization has not been included. The lower-crust partial melting curve shows that approximately 25% melt of the gabbro/amphibolite yields a composition equivalent to the low-SiO_2 granodiorites. The granodiorite fractional crystallization curve is meaningful until the granodiorite pluton is ~70% solidified, after which the magma can no longer convect. Partial melting and fractional crystallization calculations were unable to fit the tonalite data by themselves. The next section will discuss why the tonalite is likely a product of magma mixing and then fractional crystallization. Sample fractional crystallization calculations for tonalite as shown in Figures 5, 8, 11, 14, and 15 use the same bulk distribution coefficients as for granodiorite magma and one example of a starting C_0 at 50% mixing.

Multi-element variation diagrams for trace and rare earth elements are displayed in Figures 6 and 9. The calculations show that up to 10% partial melting of the mantle could yield the Escondido gabbros. Then, 25% partial melting of the lower-crust gabbro/amphibolite and up to 70% fractional crystallization of the resulting granodiorite melt could yield the Escondido granodiorites.

MAGMA MIXING

Partial Melting and Fractional Crystallization as Insufficient

The foregoing calculations provide scenarios for producing some of the Escondido plutons. However, partial melting and fractional crystallization separately or in combination are not sufficient to explain the full range of gabbros, tonalites, and granodiorites. This lack has been noted in the case of other magma geochemistry as well (see, e.g., Grove et al., 1982; Barnes et al., 2006).

Partial Melting

Melting calculations by themselves can explain the Escondido gabbro composition as due to 10% partial melting of the mantle as shown in Figure 6 and the granodiorite composition as due to 25% partial melting of the lower crust as shown in Figure 9, but it cannot explain the continuous range of Escondido samples.

A one-step partial melting of the mantle is not sufficient to enrich its REE composition by a factor of 100 to that found in the Escondido granodiorites (Jahn et al., 1984; Dokuz et al., 2006). Inclusion of a second-step partial melting of lower crust does not explain the trends for the Escondido tonalite and granodiorite data in such plots as MgO versus SiO_2 in Figure 8 and Co versus Ba in Figure 15.

Fractional Crystallization

Fractional crystallization can separately explain the range of compositions in the gabbros, tonalites, and granodiorites, but not the continuous range of 55%–78% SiO_2. The tonalite and granodiorite data form two separate trends and cannot be explained by a single fractional crystallization trend. Progressive fractional crystallization would yield a large volume of mafic cumulate and decreasing amounts of gabbro, tonalite, and granodiorite (Eichelberger, 1975), but in fact, the surface area exposure increases with increasing silica content. Fractional crystallization of a batch of basaltic magma from gabbro to tonalite to granodiorite cannot be the primary process in forming a batholith, as has been noted for the Sierra Nevada batholith (Reid et al., 1983; Kistler et al., 1986; Sisson et al., 1996).

Combination of Processes

A scenario might be envisioned where lower-crust gabbro/amphibolite partially melts to yield a tonalite magma that subsequently fractionally crystallizes to granodiorite. However, this presents difficulties because tonalites with low SiO_2 of 60% to 63%, cannot be generated by low-fraction partial melting of the amphibolite crust, and high-fraction partial melting is unlikely because of the massive heat budget required (Wyllie, 1977; Beard and Lofgren, 1989). Apparently partial melting and fractional crystallization must be accompanied by some other process to explain the Escondido geochemistry, and magma mixing seems to be indicated.

Evidence for Magma Mixing

For the Escondido plutons, some of the usual evidence for magma mixing is not available. Often a Sr_i versus 1/Sr plot (Kistler et al., 1986) or an initial $^{143}Nd/^{144}Nd$ versus Sr_i plot (DePaolo, 1980; McCulloch and Chappell, 1982; Barth et al., 1993) is used to demonstrate mixing (Faure, 2001), but for this study, all the data have $Sr_i < 0.704$ and show little variation. The usual petrographic evidence for magma mixing in volcanics (Eichelberger, 1975; Bloomfield and Arculus, 1989), such as reverse zoned or disequilibrium phenocrysts, banded lava, and inclusions, are minimal for the Escondido plutons; however, the physical evidence for magma mingling and mixing in plutonic complexes such as the Sierra Nevada batholith is also often negligible (Bateman, 1992; Sisson et al., 1996). Elsewhere, this lack has been explained by a significant lapse between mixing and crystallization in space and time (Feeley et al., 2002). Chemical evidence then becomes the primary indication for magma mixing.

Chemical evidence that often indicates magma mixing as a linear data array on a Harker diagram (Reid et al., 1983; Kistler et al., 1986; Frost and Mahood, 1987). Major-element data from the Escondido plutons display such a linear pattern from 50% to 75% SiO_2 in Figure 7. The results of least-squares fits to all the elements are listed in Table 5, with the correlation R^2 being high for most of the major elements, as well as the trace elements Co, Sc, V, Sr, Ba, and La. Although both restite unmixing and fractional crystallization have been argued as alternative explanations for linear Harker diagrams (Wall et al., 1987; Chappell et al., 1999), additional chemical evidence presented next also suggests magma mixing.

The most definitive method for discriminating between the magmatic processes of partial melting, mixing, and fractional crystallization is to plot the data for a compatible element against an incompatible element (Martin, 1987; Bullen and Clynne, 1990; Defant et al., 1991b). On the usual bivariate plot, a mixing line would be linear, whereas both partial melting and fractional crystallization lines would be curved with concave side up. These curves result from the incompatible element melting earlier and crystallizing later than the compatible element (Maaløe, 1985).

For the Escondido plutons, the bivariate plot of compatible Co versus incompatible Ba shown in Figure 15 does help discriminate among the three magmatic processes. The tonalite data form a separate cluster from the gabbro and granodiorite data and apparently require some third process for formation. The simplest interpretation is mixing between the other two already existing magmas, followed by fractional crystallization. Calculated curves for this scenario are shown.

Another piece of geochemical evidence for magma mixing is the relative gap in the Escondido data between 66% and 70% SiO_2. Too much low-temperature, high-viscosity felsic magma would quench a smaller volume of high-temperature, low-viscosity mafic magma before mixing could occur. Sparks and Marshall (1986) indicated that the proportion of basaltic magma must be at least 50% for mixing to occur. For this reason, Frost and Mahood (1987) found that thermal and viscosity constraints limit the composition of magma mixtures to no more than 63% SiO_2. Sisson et al. (1996) provided evidence that the quenching effect on basalt is less than they estimated, so mixing may extend up to the 66% SiO_2 in our data. Reubi and Blundy (2009) recognized a bimodality of melts ascending from the lower crust and suggested that andesites commonly result from mixing or mingling between the ascending silicic and mafic magmas in upper-crustal magmatic reservoirs to yield a SiO_2 composition of 59–66 wt%.

Finally, the major- and trace-element compositions of the Escondido tonalites are intermediate between the compositions for gabbro and granodiorite, as illustrated by comparing Figures 6 and 9. This can conveniently be explained by magma mixing, as modeled by Tatsumi and Kogiso (2003).

Magma Mixing and Tectonics

The histogram of SiO_2 in Figure 2 shows two distinctly different SiO_2 distributions between Peninsular Ranges batholith data west and east of the transition zone. The western Peninsular Ranges batholith Escondido data have a segmented SiO_2 distribution that is high in granodiorites and atypically abundant in gabbros (Chappell and Stephens, 1988) and in addition has an intermediate tonalite. The eastern Peninsular Ranges batholith data (divided by 5 to fit on the graph) are unimodal with a composition intermediate between tonalite and granodiorite.

The difference in SiO_2 distribution between west and east may be attributed to a difference in magma mixing in two different tectonic environments. Igneous rocks tend to display a bimodal SiO_2 composition during tectonic extension, whereas intermediate compositions dominate during compression (Eichelberger, 1978). If the western plutons were emplaced during tectonic extension through a thin crust, high-density mafic magma had less to inhibit ascent, low-density felsic magma could easily ascend, and intermediate magma had less time to form by mixing. If the eastern plutons were emplaced during tectonic compression through a thick crust, ascent of mafic and felsic magma would have been inhibited and the magmas would have more time to mix and yield an intermediate composition.

Recognition of the Importance of Magma Mixing

The need to explain part of the Escondido data by magma mixing is part of a general recognition of the importance of mixing (Eichelberger, 1975; Eichelberger and Gooley, 1977; Fyfe, 1982; Dufek and Bergantz, 2005). This process was suggested in the mid-nineteenth century, eclipsed in the early twentieth century by the explanatory power of fractional crystallization, and is now requiring a second look (Wilcox, 1999).

Examples of magma mixing to explain the geochemistry of plutonic complexes come from Maine (Ayuso and Arth, 1997), the Lachlan Fold Belt of Australia (Collins, 1996; Keay et al., 1997), plutons of central Idaho (Fleck and Criss, 1985; Fleck, 1990), the Coast Mountains batholith of British Columbia (Hollister and Andronicus, 2006), the Sierra Nevada batholith (Reid et al., 1983; Kistler et al., 1986; Frost and Mahood, 1987; Hill et al., 1988; Bateman, 1992; Sisson et al., 1996; Ratajeski et al., 2005), and the Peninsular Ranges batholith (DePaolo, 1980, 1981).

This mixing of basaltic and rhyolitic magma has been suggested as the primary source for andesite in volcanic-arc systems (Eichelberger, 1978; Grove et al., 1982; Reubi and Blundy, 2009). Jull and Kelemen (2001) recognized that mixing of mantle-derived basaltic and arc crust–derived silicic magmas can produce the bulk andesitic composition of continental crust, so this process is thought to be a major contributor to continental crust formation (Tatsumi, 2005).

MASS BALANCE CALCULATIONS

Mass balance calculations were used to model partial melting and fractional crystallization for the major elements (see, e.g., Ragland, 1989), using the same 10% and 25% partial melting and up to 70% fractional crystallization as previously. The compositions of initial melt, of restite or residue from partial melting, and of cumulate from fractional crystallization were taken from the data fitting described in a previous section and are listed in Table 2.

Other possible restites and cumulates for mass balance calculations are also listed in Table 2. The restite for partial melting of mantle lherzolite could be harzburgite (Brown and Mussett, 1993). The restite from partial melting of lower-crust gabbro/amphibolite could be a low-MgO garnet pyroxenite (Lee et al., 2006). Other possible compositions for this restite are a unique Escondido gabbro sample (B477) and a Green Acres gabbro sample from the eastern Peninsular Ranges batholith. Mass balance calculations show that the Green Acres gabbro is not reasonable as restite, whereas sample B477 and especially the pyroxenite are somewhat better. The composition of a cumulate from fractional crystallization of the granodiorite could be one of the atypical Escondido samples with SiO_2 between 66% and 69%, such as sample B502.

Finally, the relative volume of ultramafic residue left after partial melting of lower-crustal basalt was estimated using mass balance calculations. Since the sampling of the Escondido plutons was done on a grid, it provides accurate fractions for each pluton type: 12/67 for gabbro averaging 51.9% SiO_2, 25/67 for tonalite averaging 61.9% SiO_2, and 30/67 for granodiorite averaging 72.8% SiO_2. Using an initial lower-crustal basalt composition of 52% SiO_2 and an ultramafic residue containing 45% SiO_2, the residue would have a volume twice that of the differentiated Escondido plutons. Ratajeski et al. (2005) made a similar estimate for residues beneath the Sierra Nevada batholith and determined that the cumulates had a volume three times greater than the differentiated plutons.

PETROGENETIC MODEL

For the Escondido plutons, our petrogenetic model is based on past work (Eichelberger, 1978; Wilson, 1989; Faure, 2001; Annen et al., 2006; Lee et al., 2006) and summarized in Figure 16. The process is divided into seven steps:

Subduction

1. Slab dehydration—The subducted oceanic crust, made up of hydrothermally altered MORB, sediment, and seawater, moves to depths where it can no longer retain its hydrous mineral phases. According to Gastil et al. (1990), the underlying location where metamorphic dehydration begins and the slab loses fluids may be identified at the surface by a transition from magnetite in the western Peninsular Ranges batholith to ilmenite in the eastern Peninsular Ranges batholith.

2. Fluid migration—These slab-derived fluids migrate upward into the overlying mantle wedge. The fluids preferentially transport mobile large ion lithophile elements, but are much less enriched in immobile high field strength elements. Thus, the subduction-zone magmas are significantly enriched in Ba, Th, and U, but are much less enriched in Nb and Ta.

First Cycle: Mantle to Crust

3. Partial melting of mantle—The metasomatized ultramafic subcontinental mantle, made up of spinel lherzolite and depleted

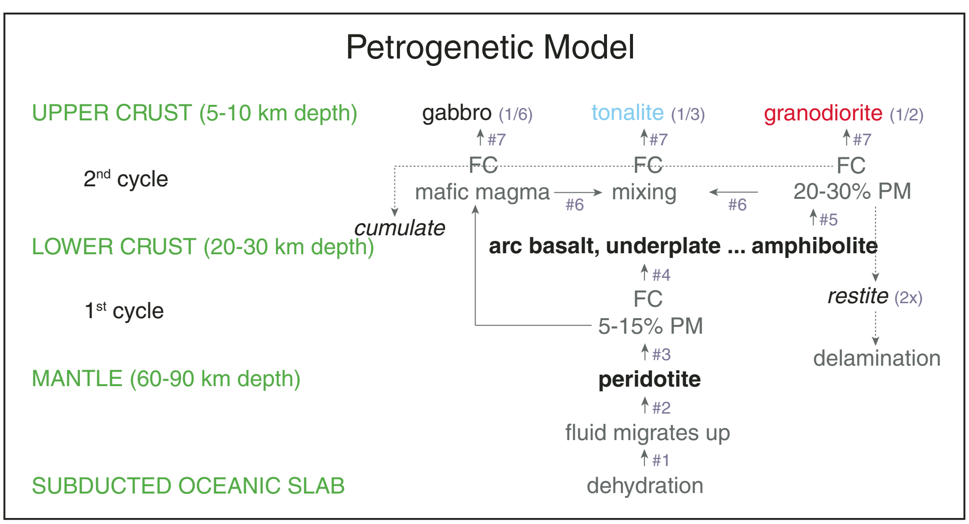

Figure 16. Petrogenetic model for generating the Escondido plutons, consisting of seven steps as described in the text. These include partial melting (PM), fractional crystallization (FC), and magma mixing in two cycles of differentiation from mantle to lower crust and lower crust to upper crust. The resulting pluton volumes are one-sixth gabbro, one-third tonalite, and one-half granodiorite. Restite from the process has a volume about twice that of the plutons.

from MORB extraction, undergoes 5%–15% partial melting due to fluid depression of the melting temperature, decompression of rising diapirs, and displacement into a deeper, higher pressure-temperature regime. The low partial melting yields hydrous mafic magmas depleted in compatible elements and enriched in incompatible elements.

4. Magma emplacement in crust—During the Triassic and Jurassic, low-Sr_i mafic magma from partial melting of the mantle erupted through the oceanic MORB crust at the western convergent margin of North America to yield the Santiago Peak arc basalts. With time, magma from the mantle also underplated the oceanic crust beneath the volcanics. This hydrous tholeiitic arc basalt is similar to MORB, but it is higher in Al_2O_3 and lower in MgO.

With tectonic extension in the Early Cretaceous, mafic magma from the mantle continued to intrude the crust or began a new surge. Some was emplaced in the upper crust and fractionally crystallized to gabbro, while the remainder provided heat to the lower crust.

Second Cycle: Lower to Upper Crust

5. Partial melting of lower crust—In Early Cretaceous time, a second cycle of differentiation began as basaltic magma from the mantle provided heat to the lower crust by conduction from underplating and advection from intrusions. The 20%–30% partial melting of the lower-crust gabbro/amphibolite generated low-Sr_i felsic magmas having a composition of the least-fractionated Woodson Mountain granodiorite. As evidenced by the Sr/Y ratios, the calc-alkaline differentiation was controlled by feldspars rather than garnets, and so it must have been above the garnet stability depth.

Partial melting of the basaltic lower crust would leave a mafic restite or residue at the base of the crust. Based on our mass balance calculations, this process would result in a volume of ultramafic rock near the crust-mantle boundary that is twice that of the Escondido plutons. Since little geophysical evidence has been found for such large volumes of high-density rock in the mantle lithosphere, it has been suggested that such cumulate or restite delaminated and sank into the mantle (Lee et al., 2007, and references therein) as long ago as the Late Cretaceous (Wells and Hoisch, 2008).

6. Magma mixing in the lower crust—Partial melting and fractional crystallization are not sufficient to explain the Escondido data; the evidence points to magma mixing as a necessary third process. Some of the granodiorite magma from partial melting of the lower crust remained in situ and mixed with gabbroic magma from the mantle to yield an intermediate tonalite magma. Magma mixing is most pronounced in a setting experiencing compression, probably in a deep-level long-lived MASH-type (melting, assimilation, storage, and homogenization) system, so the major evidence for mixing is found in the later eastern Peninsular Ranges batholith plutons.

7. Shallow-level intrusion and fractionation—The gabbro, tonalite, and granodiorite magmas derived from partial melting and mixing in the deep crust were intruded at shallow levels in the Escondido area and other parts of the western Peninsular Ranges batholith. The tonalites fractionated up to ~65% SiO_2 and the granodiorites up to 78% SiO_2, in the process concentrating incompatible and mobile elements in the final products.

SUMMARY

The data from the Escondido plutons have been used to suggest how low-Sr_i and high-SiO_2 plutons form. The model proposed involves two cycles of melting and crystallization accompanied by magma mixing: one cycle from mantle to mafic crust, a second cycle from mafic lower crust to felsic upper crust, and mixing between mafic and felsic magmas to produce intermediate-composition plutons. This model, with only two cycles, made possible quantitative melting, crystallization, mixing, and mass balance calculations to explain the Escondido data, and it sheds light on continental crust formation in general.

ACKNOWLEDGMENTS

We would like to acknowledge helpful input from Calvin Barnes, Alan Chapman, Eric Christiansen, Bill Collins, Tom Frost, Bob Martin, Robert Miller, and Jean-François Moyen.

APPENDIX 1. SAMPLE COLLECTION AND ANALYSIS METHODS

Rock samples were collected by Baird et al. (1974a, 1979) from more than 500 localities in southern California, of which more than 200 were from the Transverse Ranges and more than 300 were from the northern Peninsular Ranges batholith. The resulting data set represents one of the largest and most systematic geochemical sample sets assembled to date. The purpose of the sampling was to extract unbiased representative compositions of each pluton that could be used to determine areal distributions, with the method being similar to point counting on a microscope thin section.

A combined large- and small-scale pattern (designed by D.B. McIntyre) for sampling the southern California plutons was developed after a series of sampling studies (Baird et al., 1964, 1967a, 1967b; Morton et al., 1969). In this pattern, sample localities were spaced ~5 km apart on a grid, and at each locality, eight specimens were collected (by E.E. Welday), two at each of the four corners of a square, 400 ft (120 m) on a side. These eight specimens were combined to generate a homogeneous sample. The resulting aggregate sample for each locality might, for example, include both gabbro and tonalite specimens mixed together. The sampling technique was tested by using a grid offset by half a sample-spacing, and the results were similar. One additional "typical" sample per locality was sectioned and used to determine rock classification (Baird et al., 1979). This determination was based on an older classification system (Bateman et al., 1963) and is listed in Table A1.

Major-element geochemistry was determined by X-ray fluorescence (XRF), and the resulting analyses were published by Baird and Miesch (1984). Two splits were analyzed and compared for each location. More recently, the samples were reanalyzed using standard techniques at the U.S. Geological Survey analytical laboratories in Denver, Colorado. The major-element analyses were made by D. Siems using XRF, and the trace element analyses were made by F. Lichte using laser ablation–inductively coupled plasma–mass spectrometry

TABLE A1. DETAILS FOR THE ESCONDIDO PLUTON SAMPLES

Sample no.	Larsen*	Baird†	Rock type§	SiO_2 (wt%)	Sample no.	Larsen*	Baird†	Rock type§	SiO_2 (wt%)
B477	Kb	ga	(gbr)	46.5	B497	Kgv	qd	ton	65.9
B481	Ksm	ga	gbr	49.7	B490	Kwm	qm	(ton)	66.1
B501	Ksm	ga	gbr	49.7	B502	Kb	qd	(ton)	66.5
B483	Ksm	ga	gbr	50.1	B478	Kb	qd	(grd)	68.4
B509	Ksm	ga	gbr	50.8	B517	Kgv	qd	(grd)	68.7
B505	Ksm	ga	gbr	52.1	B493	Kim	gd	(grd)	69.4
B511	Kb	ga	gbr	52.5	B506	Kwm	gd	grd	70.7
B512	Kb	ga	gbr	52.5	B549	Klw	gd	grd	70.8
B513	Kb	qd	gbr	53.5	B542	Kwm	gd	grd	71.2
B532	Kb	ga	gbr	53.8	B472	Kwm	gd	grd	71.4
B536	Kgv	qd	gbr	53.9	B539	Kwm	gd	grd	71.7
B534	Kb	ga	gbr	54.0	B496	Kgv	qd	grd	71.7
B484	Kb	qd	ton	57.0	B540	Kwm	gd	grd	71.9
B514	Kb	qd	ton	57.0	B508	Kwm	qd	grd	71.9
B487	Kb	qd	ton	58.1	B476	Kwm	gd	grd	72.1
B523	Kb	qd	ton	58.6	B541	Kwm	gd	grd	72.1
B522	Kb	qd	ton	60.0	B520	Kwm	qd	grd	72.5
B537	Kgv	qd	ton	60.0	B538	Kwm	gd	grd	72.7
B503	Kb	qd	ton	60.5	B528	Kwm	gd	grd	72.8
B518	Ke	qd	ton	60.5	B551	Klw	gd	grd	73.0
B498	Ksm	qd	ton	61.3	B480	Kwm	gd	grd	73.7
B500	Kim	qd	ton	61.3	B479	Kwm	gd	grd	73.8
B530	Klw	qd	ton	61.3	B485	Kb	gd	grd	73.8
B531	Kb	qd	ton	61.3	B510	Kwm	gd	grd	74.2
B555	Klw	qd	ton	61.9	B475	Kwm	gd	grd	74.5
B524	Kgv	qd	ton	62.9	B504	Kwm	qm	grd	74.6
B519	Kgv	qd	ton	63.4	B489	Kwm	qm	grd	75.2
B495	Kb	qd	ton	63.5	B491	Kwm	gd	grd	75.5
B494	Kb	qd	ton	63.6	B516	Klw	gd	grd	76.0
B529	Kgv	qd	ton	63.8	B550	Klw	qm	grd	76.0
B499	Kwm	qd	ton	64.0	B482	Kwm	qm	grd	76.4
B486	Kb	qd	ton	64.1	B515	Klw	qm	grd	76.8
B544	Kb	qd	ton	64.1	B553	Klw	qm	grd	77.4
B525	Kgv	qd	ton	65.0					

Note: Samples are listed in order of increasing SiO_2 composition. Additional information about these samples is provided by Kistler et al. (2003) and in the database accompanying this volume as Table 2 in the 03-Morton folder on the CD-ROM, and in the GSA Data Repository as Item 2014040.

*Larsen (1948) units: Ksm—San Marcos gabbro, Kb—Bonsall tonalite, Kgv—Green Valley tonalite, Kwm—Woodson Mountain granodiorite, Klw—Lake Wolford granodiorite, Kim—Indian Mountain leucogranodiorite, and Ke—Escondido Creek leucogranodiorite.

†Baird et al. (1979) rock types based on the classification system of Bateman et al. (1963): ga—gabbro, qd—quartz diorite, qm—quartz monzonite, gd—granodiorite.

§Rock names used in this report: gbr—gabbro, ton—tonalite, and grd—granodiorite. Parentheses are used for atypical samples plotted with an open circle in the figures.

(ICP-MS) after sample fusion with lithium tetraborate. Because systematic differences with the earlier analyses were noted, all of the major elements were reanalyzed.

Strontium and rubidium isotope ratios (^{87}Sr/^{86}Sr and ^{87}Rb/^{86}Sr) were determined at the U.S. Geological Survey Sr isotope laboratory in Menlo Park, California (Kistler et al., 2003). Samples used for their analysis were aliquots of whole-rock powders prepared for major- and trace-element chemical analyses. Rubidium and strontium elemental abundances were determined by energy dispersive XRF methods with concentration uncertainties of ±3%. Strontium isotope ratios were determined using a MAT 261, 90° sector mass spectrometer, using the double rhenium filament mode of ionization. Strontium isotopic compositions were normalized to ^{86}Sr/^{88}Sr = 0.1194. Measurements of NBS strontium carbonate standard SRM 987 yielded a mean ^{87}Sr/^{86}Sr of 0.710239 ± 0.000015. Analytical uncertainties in ^{87}Sr/^{86}Sr values were about ±0.008%. Pb and oxygen isotope data are also available for some samples (Kistler et al., 2003; Langenheim et al., 2004).

REFERENCES CITED

Ague, J.J., and Brimhall, G.H., 1988, Magmatic arc asymmetry and distribution of anomalous plutonic belts in the batholiths of California: Effects of assimilation, crustal thickness, and depth of crystallization: Geological Society of America Bulletin, v. 100, p. 912–927, doi:10.1130/0016-7606(1988)100<0912:MAAADO>2.3.CO;2.

Allègre, C.J., and Minster, J.-F., 1978, Quantitative models of trace element behavior in magmatic processes: Earth and Planetary Science Letters, v. 38, p. 1–25, doi:10.1016/0012-821X(78)90123-1.

Annen, C., and Sparks, R.S.J., 2002, Effects of repetitive emplacement of basaltic intrusions on thermal evolution and melt generation in the crust: Earth and Planetary Science Letters, v. 203, p. 937–955, doi:10.1016/S0012-821X(02)00929-9.

Annen, C., Blundy, J.D., and Sparks, R.S.J., 2006, The genesis of intermediate and silicic magmas in deep crustal hot zones: Journal of Petrology, v. 47, no. 3, p. 505–539, doi:10.1093/petrology/egi084.

Arculus, R.J., and Powell, R., 1986, Source component mixing in the regions of arc magma generation: Journal of Geophysical Research, v. 91, no. B6, p. 5913–5926, doi:10.1029/JB091iB06p05913.

Armstrong, R.L., 1988, Mesozoic and early Cenozoic magmatic evolution of the Canadian Cordillera, *in* Clark, S.P., Burchfiel, B.C., and Suppe, J., eds., Processes in Continental Lithospheric Deformation: Geological Society of America Special Paper 218, p. 55–91.

Armstrong, R.L., Taubeneck, W.H., and Hales, P.O., 1977, Rb-Sr and K-Ar geochronometry of Mesozoic granitic rocks and their Sr isotopic composition, Oregon, Washington, and Idaho: Geological Society of America Bulletin, v. 88, p. 397–411, doi:10.1130/0016-7606(1977)88<397:RAKGOM>2.0.CO;2.

Ayuso, R.A., and Arth, J.G., 1997, The Spruce Head composite pluton: An example of mafic to silicic Salinian magmatism in coastal Maine, northern Appalachians, *in* Sinha, A.K., Whalen, J.B., and Hogan, J.P., eds., The Nature of Magmatism in the Appalachian Orogen: Geological Society of America Memoir 191, p. 19–43.

Baird, A.K., and Miesch, A.T., 1984, Batholithic Rocks of Southern California—A Model for the Petrochemical Nature of Their Source Materials: U.S. Geological Survey Professional Paper 1284, 42 p.

Baird, A.K., McIntyre, D.B., Welday, E.E., and Madlem, K.W., 1964, Chemical variations in a granitic pluton and its surrounding rocks: Science, v. 146, no. 3641, p. 258–259, doi:10.1126/science.146.3641.258.

Baird, A.K., McIntyre, D.B., and Welday, E.E., 1967a, Geochemical and structural studies in batholithic rocks of southern California: Part II. Sampling of the Rattlesnake Mountain pluton for chemical composition, variability, and trend analysis: Geological Society of America Bulletin, v. 78, p. 191–221, doi:10.1130/0016-7606(1967)78[191:GASSIB]2.0.CO;2.

Baird, A.K., McIntyre, D.B., Welday, E.E., and Morton, D.M., 1967b, A test of chemical variability and field sampling methods, Lakeview Mountain tonalite, Lakeview Mountains, southern California batholith: California Division of Mines and Geology Special Report 92, p. 11–19.

Baird, A.K., Baird, K.W., and Welday, E.E., 1974a, Chemical trends across Cretaceous batholithic rocks of southern California: Geology, v. 2, p. 493–495, doi:10.1130/0091-7613(1974)2<493:CTACBR>2.0.CO;2.

Baird, A.K., Morton, D.M., Woodford, A.O., and Baird, K.W., 1974b, Transverse Ranges Province: A unique structural-petrochemical belt across the San Andreas fault system: Geological Society of America Bulletin, v. 85, no. 2, p. 163–174, doi:10.1130/0016-7606(1974)85<163:TRPAUS>2.0.CO;2.

Baird, A.K., Baird, K.W., and Welday, E.E., 1979, Batholithic rocks of the northern Peninsular and Transverse Ranges, southern California: Chemical composition and variation, *in* Abbott, P.L., and Todd, V.R., eds., Mesozoic Crystalline Rocks: San Diego, California, San Diego State University, Department of Geological Sciences, p. 111–132.

Barnes, C.G., Allen, C.M., and Saleeby, J.B., 1986, Open- and closed-system characteristics of a tilted plutonic system, Klamath Mountains, California: Journal of Geophysical Research, v. 91, no. B6, p. 6073–6090, doi:10.1029/JB091iB06p06073.

Barnes, C.G., Mars, E.V., Swapp, S., and Frost, C.D., 2006, Petrology and geochemistry of the Middle Jurassic Ironside Mountain batholith: Evolution of potassic magmas in a primitive arc setting, *in* Snoke, A.W., and Barnes, C.G., eds., Geological Studies in the Klamath Mountains Province, California and Oregon: A Volume in Honor of William P. Irwin: Geological Society of America Special Paper 410, p. 199–221.

Barth, S., Oberli, F., Meier, M., Blattner, P., Bargossi, G.M., and Di Battistini, G., 1993, The evolution of a calc-alkaline basic to silicic magma system: Geochemical and Rb-Sr, Sm-Nd, and ^{18}O/^{16}O isotopic evidence from the late Hercynian Atesina-Cima d'Asta volcano-plutonic complex, northern Italy: Geochimica et Cosmochimica Acta, v. 57, p. 4285–4300, doi:10.1016/0016-7037(93)90323-O.

Barton, M.D., 1990, Cretaceous magmatism, metamorphism, and metallogeny in the east-central Great Basin, *in* Anderson, J.L., ed., The Nature and Origin of Cordilleran Magmatism: Geological Society of America Memoir 174, p. 283–302.

Basaltic-Volcanism-Study-Project, 1981, Basaltic Volcanism on the Terrestrial Planets: New York, Pergamon Press, 1286 p.

Bateman, P.C., 1992, Plutonism in the Central Part of the Sierra Nevada Batholith, California: U.S. Geological Survey Professional Paper 1483, 186 p.

Bateman, P.C., Clark, L.D., Huber, N.K., Moore, J.G., and Rinehart, C.D., 1963, The Sierra Nevada Batholith—A Synthesis of Recent Work across the Central Part: U.S. Geological Survey Professional Paper 414-D, 46 p.

Beard, J.S., and Lofgren, G.E., 1989, Effect of water on the composition of partial melts of greenstone and amphibolite: Science, v. 244, p. 195–197, doi:10.1126/science.244.4901.195.

Beckinsale, R.D., Sanchez-Fernandez, A.W., Brook, M., Cobbing, E.J., Taylor, W.P., and Moore, N.D., 1985, Rb-Sr whole-rock isochron and K-Ar age determinations for the Coastal batholith of Peru, *in* Pitcher, W.S., Atherton, M.P., Cobbing, E.J., and Beckinsale, R.D., eds., Magmatism at a Plate Edge: The Peruvian Andes: New York, Wiley, p. 177–202.

Bergantz, G.W., 1989, Underplating and partial melting: Implications for melt generation and extraction: Science, v. 245, p. 1093–1095, doi:10.1126/science.245.4922.1093.

Bern, A.M., Hammarstrom, J.M., Morton, D.M., Premo, W.R., and Snee, L.W., 2002, Plutonic and metamorphic rocks, northern Peninsular Ranges batholith, southern CA—Structural and uplift history based on new geobarometric and isotopic data: Geological Society of America Abstracts with Programs, v. 34, no. 6, p. 124–125.

Bloomfield, A.L., and Arculus, R.J., 1989, Magma mixing in the San Francisco volcanic field, AZ: Petrogenesis of the O'Leary Peak and Strawberry Crater volcanics: Contributions to Mineralogy and Petrology, v. 102, p. 429–453, doi:10.1007/BF00371086.

Boynton, W.V., 1984, Cosmochemistry of the rare earth elements: Meteorite studies, *in* Henderson, P., ed., Rare Earth Element Geochemistry: Developments in Geochemistry 2: Amsterdam, Netherlands, Elsevier, p. 63–114.

Brown, G.C., and Mussett, A.E., 1993, The Inaccessible Earth: An Integrated View to Its Structure and Composition: London, Chapman and Hall, 276 p.

Brown, M., and Rushmer, T., 2006, Evolution and Differentiation of the Continental Crust: Cambridge, UK, Cambridge University Press, 553 p.

Bullen, T.D., and Clynne, M.A., 1990, Trace element and isotopic constraints on magmatic evolution at Lassen volcanic center: Journal of Geophysical Research, v. 95, no. B12, p. 19,671–19,691, doi:10.1029/JB095iB12p19671.

Bussell, M.A., 1985, The centred complex of the Rio Huaura: A study of magma mixing and differentiation in high-level magma chambers, *in* Pitcher, W.S., Atherton, M.P., Cobbing, E.J., and Beckinsale, R.D., eds., Magmatism at a Plate Edge: The Peruvian Andes: New York, Wiley, p. 128–155.

Chappell, B.W., and Stephens, W.E., 1988, Origin of infracrustal (I-type) granite magmas: Transactions of the Royal Society of Edinburgh–Earth Sciences, v. 79, p. 71–86, doi:10.1017/S0263593300014139.

Chappell, B.W., White, A.J.R., Williams, I.S., Wyborn, D., Hergt, J.M., Woodhead, J.D., and Collins, W.J., 1999, Discussion and reply: Evaluation of petrogenetic models for Lachlan Fold Belt granitoids: Implications for crustal architecture and tectonic models: Australian Journal of Earth Sciences, v. 46, p. 827–836, doi:10.1046/j.1440-0952.1999.00742.x.

Collins, W.J., 1996, Lachlan Fold Belt granitoids: Products of three-component mixing, *in* Brown, M., Candela, P.A., Peck, D.L., Stephens, W.E., Walker, R.J., and Zen, E.-a., eds., The Third Hutton Symposium on the Origin of Granites and Related Rocks: Geological Society of America Special Paper 315, p. 171–181.

Conrey, R.M., Hooper, P.R., Larson, P.B., Chesley, J.T., and Ruiz, J., 2001, Trace element and isotopic evidence for two types of crustal melting beneath a High Cascade volcanic center, Mt. Jefferson, Oregon: Contributions to Mineralogy and Petrology, v. 141, p. 710–732, doi:10.1007/s004100100259.

Criscione, J.J., Davis, T.E., and Ehlig, P.L., 1978, The age of sedimentation/diagenesis for the Bedford Canyon Formation and the Santa Monica Formation in southern California: A Rb/Sr evaluation, *in* Howell, D.G., and McDougall, K.A., eds., Mesozoic Paleogeography of the Western United States: Pacific Coast Paleogeography Symposium 2: Los Angeles, California, Pacific Section, Society of Economic Paleontologists and Mineralogists, p. 385–396.

Criss, R.E., and Fleck, R.J., 1987, Petrogenesis, geochronology, and hydrothermal systems of the northern Idaho batholith and adjacent areas based on $^{18}O/^{16}O$, D/H, $^{87}Sr/^{86}Sr$, K-Ar, and $^{40}Ar/^{39}Ar$ studies, *in* Vallier, T.L., and Brooks, H.C., eds., Geology of the Blue Mountains Region of Oregon, Idaho, and Washington: The Idaho Batholith and Its Border Zone: U.S. Geological Survey Professional Paper 1436, p. 95–137.

Cruden, A.R., 2006, Emplacement and growth of plutons: Implications for rates of melting and mass transfer in continental crust, *in* Brown, M., and Rushmer, T., eds., Evolution and Differentiation of the Continental Crust: Cambridge, UK, Cambridge University Press, p. 455–519.

Davidson, J.P., and Arculus, R.J., 2006, The significance of Phanerozoic arc magmatism in generating continental crust, *in* Brown, M., and Rushmer, T., eds., Evolution and Differentiation of the Continental Crust: Cambridge, UK, Cambridge University Press, p. 135–172.

Davidson, J.P., Turner, S.P., Handley, H.K., Macpherson, C.G., and Dosseto, A., 2007, Amphibole "sponge" in arc crust?: Geology, v. 35, no. 9, p. 787–790, doi:10.1130/G23637A.1.

Defant, M.J., and Drummond, M.S., 1990, Derivation of some modern arc magmas by melting of young subducted lithosphere: Nature, v. 347, p. 662–665, doi:10.1038/347662a0.

Defant, M.J., Clark, L.F., Stewart, R.H., Drummond, M.S., de Boer, J.Z., Maury, R.C., Bellon, H., Jackson, T.E., and Restrepo, J.F., 1991a, Andesite and dacite genesis via contrasting processes: The geology and geochemistry of El Valle Volcano, Panama: Contributions to Mineralogy and Petrology, v. 106, p. 309–324, doi:10.1007/BF00324560.

Defant, M.J., Maury, R.C., Ripley, E.M., Feigenson, M.D., and Jacques, D., 1991b, An example of island-arc petrogenesis: Geochemistry and petrology of the southern Luzon arc, Philippines: Journal of Petrology, v. 32, no. 3, p. 455–500, doi:10.1093/petrology/32.3.455.

DePaolo, D.J., 1980, Sources of continental crust: Neodymium isotope evidence from the Sierra Nevada and Peninsular Ranges: Science, v. 209, p. 684–687, doi:10.1126/science.209.4457.684.

DePaolo, D.J., 1981, A neodymium and strontium isotopic study of the Mesozoic calc-alkaline granitic batholiths of the Sierra Nevada and Peninsular Ranges, California: Journal of Geophysical Research, v. 86, no. B11, p. 10,470–10,488, doi:10.1029/JB086iB11p10470.

Dokuz, A., Tanyolu, E., and Genç, S., 2006, A mantle- and a lower crust–derived bimodal suite in the Yusufeli (Artvin) area, NE Turkey: Trace element and REE evidence for subduction-related rift origin of Early Jurassic Demirkent intrusive complex: International Journal of Earth Sciences, v. 95, p. 370–394, doi:10.1007/s00531-005-0046-6.

Drummond, M.S., Wesolowski, D., and Allison, D.T., 1988, Generation, diversification, and emplacement of the Rockford Granite, Alabama Appalachians: Mineralogic, petrologic, isotopic (C & O), and P-T constraints: Journal of Petrology, v. 29, no. 4, p. 869–897, doi:10.1093/petrology/29.4.869.

Dufek, J., and Bergantz, G.W., 2005, Lower crustal magma genesis and preservation: A stochastic framework for the evaluation of basalt-crust interaction: Journal of Petrology, v. 46, no. 11, p. 2167–2195, doi:10.1093/petrology/egi049.

DuFrane, S.A., Asmerom, Y., Mukasa, S.B., Morris, J.D., and Dreyer, B.M., 2006, Subduction and melting processes inferred from U-series, Sr-Nd-Pb isotope, and trace element data, Bicol and Bataan arcs, Philippines: Geochimica et Cosmochimica Acta, v. 70, p. 3401–3420, doi:10.1016/j.gca.2006.04.020.

Eby, G.N., 1990, The A-type granitoids: A review of their occurrence and chemical characteristics and speculations on their petrogenesis: Lithos, v. 26, p. 115–134, doi:10.1016/0024-4937(90)90043-Z.

Eby, G.N., Krueger, H.W., and Creasy, J.W., 1992, Geology, geochronology, and geochemistry of the White Mountain batholith, New Hampshire, *in* Puffer, J.H., and Ragland, P.C., eds., Eastern North American Mesozoic Magmatism: Geological Society of America Special Paper 268, p. 379–397.

Eichelberger, J.C., 1975, Origin of andesite and dacite: Evidence of mixing at Glass Mountain in California and at other circum-Pacific volcanoes: Geological Society of America Bulletin, v. 86, p. 1381–1391, doi:10.1130/0016-7606(1975)86<1381:OOAADE>2.0.CO;2.

Eichelberger, J.C., 1978, Andesitic volcanism and crustal evolution: Nature, v. 275, p. 21–27, doi:10.1038/275021a0.

Eichelberger, J.C., and Gooley, R., 1977, Evolution of silicic magma chambers and their relationship to basaltic volcanism, *in* Heacock, J.G., Keller, G.V., Oliver, J.E., and Simmons, G., eds., The Earth's Crust: Its Nature and Physical Properties: American Geophysical Union Geophysical Monograph 20, p. 57–77.

Ernst, W.G., 1990, Metamorphism in allochthonous and autochthonous terranes of the western United States: Philosophical Transactions of the Royal Society of London, ser. A, v. 331, p. 549–570, doi:10.1098/rsta.1990.0089.

Ewart, A., 1982, The mineralogy and petrology of Tertiary-Recent orogenic volcanic rocks: With special reference to the andesitic-basaltic compositional range, *in* Thorpe, R.S., ed., Andesites: Orogenic Andesites and Related Rocks: New York, Wiley, p. 25–95.

Faure, G., 1986, Principles of Isotope Geology: New York, Wiley, 589 p.

Faure, G., 2001, Origin of Igneous Rocks: The Isotopic Evidence: New York, Springer-Verlag, 496 p.

Faure, G., and Mensing, T.M., 2005, Isotopes: Principles and Applications: Hoboken, New Jersey, John Wiley, 897 p.

Faure, G., and Powell, J.L., 1972, Strontium Isotope Geology: Minerals, Rocks and Inorganic Materials 5: New York, Springer-Verlag, 188 p.

Feeley, T.C., Cosca, M.A., and Lindsay, C.R., 2002, Petrogenesis and implications of calc-alkaline cryptic hybrid magmas from Washburn Volcano, Absaroka volcanic province, USA: Journal of Petrology, v. 43, p. 663–703, doi:10.1093/petrology/43.4.663.

Fitches, W.R., Graham, R.H., Hussein, I.M., Ries, A.C., Shackleton, R.M., and Price, R.C., 1983, The late Proterozoic ophiolite of Sol Hamed, NE Sudan: Precambrian Research, v. 19, p. 385–411, doi:10.1016/0301-9268(83)90022-0.

Fleck, R.J., 1990, Neodymium, strontium, and trace-element evidence of crustal anatexis and magma mixing in the Idaho batholith, *in* Anderson, J.L., ed., The Nature and Origin of Cordilleran Magmatism: Geological Society of America Memoir 174, p. 359–373.

Fleck, R.J., and Criss, R.E., 1985, Strontium and oxygen isotopic variations in Mesozoic and Tertiary plutons of central Idaho: Contributions to Mineralogy and Petrology, v. 90, p. 291–308, doi:10.1007/BF00378269.

Frost, B.R., and Frost, C.D., 2008, A geochemical classification for feldspathic igneous rocks: Journal of Petrology, v. 49, no. 11, p. 1955–1969, doi:10.1093/petrology/egn054.

Frost, T.P., and Mahood, G.A., 1987, Field, chemical, and physical constraints on mafic-felsic magma interaction in the Lamarck Granodiorite, Sierra Nevada, California: Geological Society of America Bulletin, v. 99, p. 272–291, doi:10.1130/0016-7606(1987)99<272:FCAPCO>2.0.CO;2.

Fullagar, P.D., and Butler, J.R., 1979, 325 to 265 m.y.-old granitic plutons in the Piedmont of the southeastern Appalachians: American Journal of Science, v. 279, p. 161–185, doi:10.2475/ajs.279.2.161.

Fyfe, W.S., 1982, Andesites—Product of geosphere mixing, *in* Thorpe, R.S., ed., Andesites: Orogenic Andesites and Related Rocks: New York, Wiley, p. 663–667.

Gastil, R.G., Diamond, J.L., Knaack, C.M., Walawender, M.J., Marshall, M., Boyles, C., Chadwick, B., and Erskine, B.G., 1990, The problem of the magnetite/ilmenite boundary in southern and Baja California, California, *in* Anderson, J.L., ed., The Nature and Origin of Cordilleran Magmatism: Geological Society of America Memoir 174, p. 19–32.

Gill, J.B., 1981, Orogenic Andesites and Plate Tectonics: Minerals and Rocks 16: New York, Springer-Verlag, 390 p.

Greene, A.R., DeBari, S.M., Kelemen, P.B., Blusztajn, J., and Clift, P.D., 2006, A detailed geochemical study of island arc crust: The Talkeetna arc section, south-central Alaska: Journal of Petrology, v. 47, no. 6, p. 1051–1093, doi:10.1093/petrology/egl002.

Grégoire, M., Bell, D.R., and Le Roex, A.P., 2003, Garnet lherzolites from the Kaapvaal craton (South Africa): Trace element evidence for a metasomatic history: Journal of Petrology, v. 44, no. 4, p. 629–657, doi:10.1093/petrology/44.4.629.

Gromet, L.P., and Silver, L.T., 1987, REE variations across the Peninsular Ranges batholith: Implications for batholithic petrogenesis and crustal growth in magmatic arcs: Journal of Petrology, v. 28, p. 75–125, doi:10.1093/petrology/28.1.75.

Grove, T.L., Gerlach, D.C., and Sando, T.W., 1982, Origin of calc-alkaline series lavas at Medicine Lake volcano by fractionation, assimilation and mixing: Contributions to Mineralogy and Petrology, v. 80, p. 160–182, doi:10.1007/BF00374893.

Grove, T.L., Elkins-Tanton, L.T., Parman, S.W., Chatterjee, N., Müntener, O., and Gaetani, G.A., 2003, Fractional crystallization and mantle-melting controls on calc-alkaline differentiation trends: Contributions to Mineralogy and Petrology, v. 145, p. 515–533, doi:10.1007/s00410-003-0448-z.

Hart, S.R., Brooks, C., Krogh, T.E., Davis, G.L., and Nava, D., 1970, Ancient and modern volcanic rocks: A trace element model: Earth and Planetary Science Letters, v. 10, p. 17–28, doi:10.1016/0012-821X(70)90060-9.

Hawkesworth, C.J., and Kemp, A.I.S., 2006, The differentiation and rates of generation of the continental crust: Chemical Geology, v. 226, p. 134–143, doi:10.1016/j.chemgeo.2005.09.017.

Hawkesworth, C.J., O'Nions, R.K., Pankhurst, R.J., Hamilton, P.J., and Evensen, N.M., 1977, A geochemical study of island-arc and back-arc tholeiites from the Scotia Sea: Earth and Planetary Science Letters, v. 36, p. 253–262, doi:10.1016/0012-821X(77)90207-2.

Herzig, C.T., 1991, Petrogenetic and Tectonic Development of the Santiago Peak Volcanics, Northern Santa Ana Mountains, California [Ph.D. thesis]: Riverside, University of California, 376 p.

Herzig, C.T., and Kimbrough, D.L., 2014, this volume, Santiago Peak Volcanics: Early Cretaceous arc volcanism of the western Peninsular Ranges batholith, southern California, *in* Morton, D.M., and Miller, F.K., eds., Peninsular Ranges Batholith, Baja California and Southern California: Geological Society of America Memoir 211, doi:10.1130/2014.1211(09).

Hill, M., O'Neil, J.R., Noyes, H., Frey, F.A., and Wones, D.R., 1988, Sr, Nd and O isotope variations in compositionally zoned and unzoned plutons in the central Sierra Nevada batholith: American Journal of Science, v. 288-A, p. 213–241.

Hollister, L.S., and Andronicus, C.L., 2006, Formation of new continental crust in western British Columbia during transpression and transtension: Earth and Planetary Science Letters, v. 249, p. 29–38, doi:10.1016/j.epsl.2006.06.042.

Huppert, H.E., and Sparks, R.S.J., 1988, The generation of granitic magmas by intrusion of basalt into continental crust: Journal of Petrology, v. 29, no. 3, p. 599–624, doi:10.1093/petrology/29.3.599.

Jachens, R.C., and Morton, D.M., 1991, Geophysical studies in the Southern California Areal Mapping Project (SCAMP): Geological Society of America Abstracts with Programs, v. 23, no. 5, p. 476.

Jahn, B.-m., Vidal, P., and Kröner, A., 1984, Multi-chronometric ages and origin of Archaean tonalitic gneisses in Finnish Lapland: A case for long crustal residence time: Contributions to Mineralogy and Petrology, v. 86, p. 398–408, doi:10.1007/BF01187143.

James, D.E., 1981, The combined use of oxygen and radiogenic isotopes as indicators of crustal contamination: Annual Review of Earth and Planetary Sciences, v. 9, p. 311–344, doi:10.1146/annurev.ea.09.050181.001523.

Jull, M., and Kelemen, P.B., 2001, On the conditions for lower crustal convective instability: Journal of Geophysical Research, v. 106, no. B4, p. 6423–6446, doi:10.1029/2000JB900357.

Kamiyama, H., Nakajima, T., and Kamioka, H., 2007, Magmatic stratigraphy of the tilted Tottabetsu plutonic complex, Hokkaido, north Japan: Magma chamber dynamics and pluton construction: The Journal of Geology, v. 115, p. 295–314, doi:10.1086/512754.

Kay, R.W., Sun, S.-s., and Lee-Hu, C.-N., 1978, Pb and Sr isotopes in volcanic rocks from the Aleutian Islands and Pribilof Islands, Alaska: Geochimica et Cosmochimica Acta, v. 42, p. 263–273, doi:10.1016/0016-7037(78)90178-3.

Kay, S.M., Kay, R.W., Brueckner, H.K., and Rubenstone, J.L., 1983, Tholeiitic Aleutian arc plutonism: The Finger Bay pluton, Adak, Alaska: Contributions to Mineralogy and Petrology, v. 82, p. 99–116, doi:10.1007/BF00371179.

Keay, S., Collins, W.J., and McCulloch, M.T., 1997, A three-component Sr-Nd isotopic mixing model for granitoid genesis, Lachlan fold belt, eastern Australia: Geology, v. 25, no. 4, p. 307–310, doi:10.1130/0091-7613(1997)025<0307:ATCSNI>2.3.CO;2.

Kelemen, P.B., Yogodzinski, G.M., and Scholl, D.W., 2003, Along-strike variation in the Aleutian Island arc: Genesis of high Mg# andesite and implications for continental crust, *in* Eiler, J., ed., Inside the Subduction Factory: American Geophysical Union Geophysical Monograph 138, p. 223–276.

Kistler, R.W., and Morton, D.M., 1994, Sr, Rb, Sr_i variation, and whole-rock Rb/Sr ages of plutons in the northern Peninsular Ranges batholith, southern California: Geological Society of America Abstracts with Programs, v. 26, no. 2, p. 63.

Kistler, R.W., and Peterman, Z.E., 1978, Reconstruction of Crustal Blocks of California on the Basis of Initial Strontium Isotopic Compositions of Mesozoic Granitic Rocks: U.S. Geological Survey Professional Paper 1071, 17 p.

Kistler, R.W., Chappell, B.W., Peck, D.L., and Bateman, P.C., 1986, Isotopic variation in the Tuolumne Intrusive Suite, central Sierra Nevada, California: Contributions to Mineralogy and Petrology, v. 94, p. 205–220, doi:10.1007/BF00592937.

Kistler, R.W., Wooden, J.L., and Morton, D.M., 2003, Isotopes and Ages in the Northern Peninsular Ranges Batholith, Southern California: U.S. Geological Survey Open-File Report 03-489, 45 p.

Kodaira, S., Sato, T., Takahashi, N., Miura, S., Tamura, Y., Tatsumi, Y., and Kaneda, Y., 2007, New seismological constraints on growth of continental crust in the Izu-Bonin intra-oceanic arc: Geology, v. 35, no. 11, p. 1031–1034, doi:10.1130/G23901A.1.

Krummenacher, D., Gastil, R.G., Bushee, J., and Doupont, J., 1975, K-Ar apparent ages, Peninsular Ranges batholith, southern California and Baja California: Geological Society of America Bulletin, v. 86, p. 760–768, doi:10.1130/0016-7606(1975)86<760:KAAPRB>2.0.CO;2.

Kuno, H., 1968, Differentiation of basalt magmas, *in* Hess, H.H., and Poldervaart, A., eds., Basalts: The Poldervaart Treatise on Rocks of Basaltic Composition 2: New York, Interscience (Wiley), p. 623–688.

Langenheim, V.E., Jachens, R.C., Morton, D.M., Kistler, R.W., and Matti, J.C., 2004, Geophysical and isotopic mapping of preexisting crustal structures that influenced the location and development of the San Jacinto fault zone, southern California: Geological Society of America Bulletin, v. 116, no. 9/10, p. 1143–1157, doi:10.1130/B25277.1.

Larsen, E.S., 1948, Batholith and Associated Rocks of Corona, Elsinore, and San Luis Rey Quadrangles, Southern California: Geological Society of America Memoir 29, 182 p.

Leat, P.T., and Larter, R.D., 2003, Intra-oceanic subduction systems: Introduction, *in* Larter, R.D., and Leat, P.T., eds., Intra-Oceanic Subduction Systems: Tectonic and Magmatic Processes: Geological Society of London Special Publication 219, p. 1–17.

Lee, C.-T.A., Cheng, X., and Horodyskyj, U., 2006, The development and refinement of continental arcs by primary basaltic magmatism, garnet pyroxenite accumulation, basaltic recharge and delamination: Insights from the Sierra Nevada, California: Contributions to Mineralogy and Petrology, v. 151, p. 222–242, doi:10.1007/s00410-005-0056-1.

Lee, C.-T.A., Morton, D.M., Kistler, R.W., and Baird, A.K., 2007, Petrology and tectonics of Phanerozoic continent formation: From island arcs to accretion and continental arc magmatism: Earth and Planetary Science Letters, v. 263, p. 370–387, doi:10.1016/j.epsl.2007.09.025.

Le Maitre, R.W., 2002, Igneous Rocks: IUGS Classification and Glossary: Recommendations of the International Union of Geological Sciences, Subcommission on the Systematics of Igneous Rocks: Cambridge, UK, Cambridge University Press, 236 p.

Maaløe, S., 1985, Principles of Igneous Petrology: New York, Springer-Verlag, 374 p.

Maaløe, S., and Aoki, K.-i., 1977, The major element composition of the upper mantle estimated from the composition of lherzolites: Contributions to Mineralogy and Petrology, v. 63, p. 161–173, doi:10.1007/BF00398777.

Machida, S., Ishii, T., Kimura, J.-I., Awaji, S., and Kato, Y., 2008, Petrology and geochemistry of cross-chains in the Izu-Bonin back arc: Three mantle components with contributions of hydrous liquids from a deeply subducted slab: Geochemistry Geophysics Geosystems, v. 9, no. 5, Q05002, doi:10.1029/2007GC001641.

Magaritz, M., Whitford, D.J., and James, D.E., 1978, Oxygen isotopes and the origin of high-$^{87}Sr/^{86}Sr$ andesites: Earth and Planetary Science Letters, v. 40, p. 220–230, doi:10.1016/0012-821X(78)90092-4.

Martin, H., 1987, Petrogenesis of Archaean trondhjemites, tonalites, and granodiorites from eastern Finland: Major Nd trace element geochemistry: Journal of Petrology, v. 28, no. 5, p. 921–953, doi:10.1093/petrology/28.5.921.

McCulloch, M.T., and Chappell, B.W., 1982, Nd isotopic characteristics of S- and I-type granites: Earth and Planetary Science Letters, v. 58, p. 51–64, doi:10.1016/0012-821X(82)90102-9.

McLennan, S.M., Taylor, S.R., and Hemming, S.R., 2006, Composition, differentiation, and evolution of continental crust: Constraints from sedimentary rocks and heat flow, *in* Brown, M., and Rushmer, T., eds., Evolution and Differentiation of the Continental Crust: Cambridge, UK, Cambridge University Press, p. 92–134.

Meen, J.K., 1990, Elevation of potassium content of basaltic magma by fractional crystallization: The effect of pressure: Contributions to Mineralogy and Petrology, v. 104, p. 309–331, doi:10.1007/BF00321487.

Middlemost, E.A.K., 1989, Iron oxidation ratios, norms and the classification of volcanic rocks: Chemical Geology, v. 77, p. 19–26, doi:10.1016/0009-2541(89)90011-9.

Mikoshiba, M.U., Takahashi, Y., Takahashi, Y., Kausar, A.B., Khan, T., Kubo, K., and Shirahase, T., 1999, Rb-Sr isotopic study of the Chilas igneous complex, Kohistan, northern Pakistan, *in* Macfarlane, A., Sorkhabi, R.B., and Quade, J., eds., Himalaya and Tibet: Mountain Roots to Mountain Tops: Geological Society of America Special Paper 328, p. 47–57.

Miyashiro, A., 1974, Volcanic rock series in island arcs and active continental margins: American Journal of Science, v. 274, p. 321–355, doi:10.2475/ajs.274.4.321.

Morton, D.M., and Kistler, R.W., 1997, Sr_i variation in the northern Peninsular Ranges batholith: Geological Society of America Abstracts with Programs, v. 29, no. 6, p. 69.

Morton, D.M., and Miller, F.K., 1987, K/Ar apparent ages of plutonic rocks from the northern part of the Peninsular Ranges batholith, southern California: Geological Society of America Abstracts with Programs, v. 19, no. 6, p. 435.

Morton, D.M., Baird, A.K., and Baird, K.W., 1969, The Lakeview Mountains pluton, southern California batholith: Part II. Chemical composition and variation: Geological Society of America Bulletin, v. 80, p. 1553–1564, doi:10.1130/0016-7606(1969)80[1553:TLMPSC]2.0.CO;2.

Morton, D.M., Alvarez, R.M., Alcott, A., Miller, F.K., and Cossette, P.M., 2014, this volume, Subduction transitioning from beneath oceanic crust to beneath continental crust, northern Peninsular Ranges batholith, *in* Morton, D.M., and Miller, F.K., eds., Peninsular Ranges Batholith, Baja California and Southern California: Geological Society of America Memoir 211, doi:10.1130/2014.1211(13).

Moyen, J.-F., and Stevens, G., 2006, Experimental constraints on TTG petrogenesis: Implications for Archean geodynamics, *in* Benn, K., Mareschal, J.-C., and Condie, K.C., eds., Archean Geodynamics and Environments: American Geophysical Union Geophysical Monograph 164, p. 149–175, doi:10.1029/164GM11.

Neumann, E.-R., 1980, Petrogenesis of the Oslo region larvikites and associated rocks: Journal of Petrology, v. 21, no. 3, p. 499–531, doi:10.1093/petrology/21.3.499.

Pearce, J.A., 1983, Role of the sub-continental lithosphere in magma genesis at active continental margins, *in* Hawkesworth, C.J., and Norry, M.J., eds., Continental Basalts and Mantle Xenoliths: Cheshire, UK, Shiva, p. 230–249.

Pearce, J.A., and Parkinson, I.J., 1993, Trace element models for mantle melting: Application to volcanic arc petrogenesis, *in* Prichard, H.M., Alabaster, T., Harris, N.B.W., and Neary, C.R., eds., Magmatic Processes and Plate Tectonics: Geological Society of London Special Publication 76, p. 373–403.

Pearce, J.A., Harris, N.B.W., and Tindle, A.G., 1984, Trace element discrimination diagrams for the tectonic interpretation of granitic rocks: Journal of Petrology, v. 25, p. 956–983, doi:10.1093/petrology/25.4.956.

Pearcy, L.G., DeBari, S.M., and Sleep, N.H., 1990, Mass balance calculations for two sections of island arc crust and implications for the formation of continents: Earth and Planetary Science Letters, v. 96, p. 427–442, doi:10.1016/0012-821X(90)90018-S.

Perfit, M.R., Gust, D.A., Bence, A.E., Arculus, R.J., and Taylor, S.R., 1980, Chemical characteristics of island-arc basalts: Implications for mantle sources: Chemical Geology, v. 30, p. 227–256.

Petford, N., and Gallagher, K., 2001, Partial melting of mafic (amphibolitic) lower crust by periodic influx of basaltic magma: Earth and Planetary Science Letters, v. 193, p. 483–499, doi:10.1016/S0012-821X(01)00481-2.

Petford, N., Cruden, A.R., McCaffrey, K.J.W., and Vigneresse, J.L., 2000, Granite magma formation, transport and emplacement in the Earth's crust: Nature, v. 408, p. 669–673, doi:10.1038/35047000.

Premo, W.R., Morton, D.M., Snee, L.W., Naeser, N.D., and Fanning, C.M., 1998, Isotopic ages, cooling histories, and magmatic origins for Mesozoic tonalitic plutons from the N. Peninsular Ranges batholith, S. California: Geological Society of America Abstracts with Programs, v. 30, no. 5, p. 59–60.

Premo, W.R., Morton, D.M., Snee, L.W., and Bern, A.M., 2002, SHRIMP U-Pb ages of provenance from detrital zircon populations of intra-batholithic metasedimentary rock, N. Peninsular Ranges batholith, southern California: Implications for their tectonic setting: Geological Society of America Abstracts with Programs, v. 34, no. 6, p. 124.

Ragland, P.C., 1989, Basic Analytical Petrology: Oxford, UK, Oxford University Press, 369 p.

Ratajeski, K., Sisson, T.W., and Glazner, A.F., 2005, Experimental and geochemical evidence for derivation of the El Capitan Granite, California, by partial melting of hydrous gabbroic lower crust: Contributions to Mineralogy and Petrology, v. 149, p. 713–734, doi:10.1007/s00410-005-0677-4.

Reid, J.B., Evans, O.C., and Fates, D.G., 1983, Magma mixing in granitic rocks of the central Sierra Nevada, California: Earth and Planetary Science Letters, v. 66, p. 243–261, doi:10.1016/0012-821X(83)90139-5.

Reubi, O., and Blundy, J.D., 2009, A dearth of intermediate melts at subduction zone volcanoes and the petrogenesis of arc andesites: Nature, v. 461, p. 1269–1273, doi:10.1038/nature08510.

Rogers, T.H., 1965, Geologic Map of California, Santa Ana Sheet: Sacramento, California Department of Conservation, Division of Mines and Geology, scale 1:250,000.

Rollinson, H.R., 1993, Using Geochemical Data: Evaluation, Presentation, Interpretation, Longman Geochemistry Series: Edinburgh Gate, UK, Longman, 352 p.

Rudnick, R.L., 1995, Making continental crust: Nature, v. 378, p. 571–578, doi:10.1038/378571a0.

Saunders, A.D., and Tarney, J., 1984, Geochemical characteristics of basaltic volcanism within back-arc basins, *in* Kokelaar, B.P., and Howells, M.F., eds., Marginal Basin Geology: Volcanic and Associated Sedimentary and Tectonic Processes in Modern and Ancient Marginal Basins: Geological Society of London Special Publication 16, p. 59–76.

Schmidt, K.L., Wetmore, P.H., Johnson, S.E., and Paterson, S.R., 2002, Controls on orogenesis along an ocean-continent margin transition in the Jura-Cretaceous Peninsular Ranges batholith, *in* Barth, A.P., ed., Contributions to Crustal Evolution of the Southwestern United States: Geological Society of America Special Paper 365, p. 49–71.

Silver, L.T., and Chappell, B.W., 1988, The Peninsular Ranges batholith: An insight into the evolution of the Cordilleran batholiths of southwestern North America: Transactions of the Royal Society of Edinburgh–Earth Sciences, v. 79, p. 105–121, doi:10.1017/S0263593300014152.

Silver, L.T., Taylor, H.P., and Chappell, B.W., 1979, Some petrological, geochemical and geochronological observations of the Peninsular Ranges batholith near the international border of the U.S.A. and Mexico, *in* Abbott, P.L., and Todd, V.R., eds., Mesozoic Crystalline Rocks: San Diego, California, San Diego State University, Department of Geological Sciences, p. 83–110.

Sisson, T.W., Grove, T.L., and Coleman, D.S., 1996, Hornblende gabbro sill complex at Onion Valley, California, and a mixing origin for the Sierra Nevada batholith: Contributions to Mineralogy and Petrology, v. 126, p. 81–108, doi:10.1007/s004100050237.

Sisson, T.W., Ratajeski, K., Hankins, W.B., and Glazner, A.F., 2005, Voluminous granitic magmas from common basaltic sources: Contributions to Mineralogy and Petrology, v. 148, p. 635–661, doi:10.1007/s00410-004-0632-9.

Snoke, A.W., and Barnes, C.G., eds., 2006, Geological Studies in the Klamath Mountains Province, California and Oregon: A Volume in Honor of William P. Irwin: Geological Society of America Special Paper 410, 505 p.

Sparks, R.S.J., and Marshall, L.A., 1986, Thermal and mechanical constraints on mixing between mafic and silicic magmas: Journal of Volcanology and Geothermal Research, v. 29, p. 99–124, doi:10.1016/0377-0273(86)90041-7.

Stern, R.J., Fouch, M.J., and Klemperer, S.L., 2003, An overview of the Izu-Bonin-Mariana subduction factory, *in* Eiler, J., ed., Inside the Subduction

Factory: American Geophysical Union Geophysical Monograph 138, p. 175–222, doi: 10.1029/138GM10.
Stevens, G., and Moyen, J.-F., 2007, Metamorphism in the Barberton Granite Greenstone Terrain: A record of Paleoarchean accretion, *in* van Kranendonk, M.J., Smithies, R.H., and Bennett, V.C., eds., Earth's Oldest Rocks: Developments in Precambrian Geology 15: Amsterdam, Elsevier, p. 669–698, doi:10.1016/S0166-2635(07)15057-X.
Strand, R.G., 1962, Geologic Map of California, San Diego—El Centro Sheet: San Francisco, California Department of Conservation, Division of Mines and Geology, scale 1:250,000.
Sun, S.-s., 1980, Lead isotopic study of young volcanic rocks from mid-ocean ridges, ocean islands and island arcs: Philosophical Transactions of the Royal Society of London, ser. A, v. 297, p. 409–445, doi:10.1098/rsta.1980.0224.
Sun, S.-s., and McDonough, W.F., 1989, Chemical and isotopic systematics of oceanic basalts: Implications for mantle composition and processes, *in* Saunders, A.D., and Norry, M.J., eds., Magmatism in the Ocean Basins: Geological Society of London Special Publication 42, p. 313–345.
Symons, D.T.A., Walawender, M.J., Smith, T.E., Molnar, S.E., Harris, M.J., and Blackburn, W.H., 2003, Paleomagnetism and geobarometry of the La Posta pluton, California, *in* Johnson, S.E., Paterson, S.R., Fletcher, J.M., Girty, G.H., Kimbrough, D.L., and Martín-Barajas, A., eds., Tectonic Evolution of Northwestern México and the Southwestern USA: Geological Society of America Special Paper 374, p. 135–155.
Tanaka, H., Smith, T.E., and Huang, C.H., 1984, The Santiago Peak volcanic rocks of the Peninsular Ranges batholith, southern California: Volcanic rocks associated with coeval gabbros: Bulletin of Volcanology, v. 47, no. 1, p. 153–171, doi:10.1007/BF01960546.
Tatsumi, Y., 2005, The subduction factory: How it operates in the evolving Earth: GSA Today, v. 15, no. 7, p. 4–10, doi:10.1130/1052-5173(2005)015[4:TSFHIO]2.0.CO;2.
Tatsumi, Y., and Kogiso, T., 2003, The subduction factory: Its role in the evolution of the Earth's crust and mantle, *in* Larter, R.D., and Leat, P.T., eds., Intra-Oceanic Subduction Systems: Tectonic and Magmatic Processes: Geological Society of London Special Publication 219, p. 55–80.
Taylor, H.P., and Silver, L.T., 1978, Oxygen isotope relationships in plutonic igneous rocks of the Peninsular Ranges batholith, southern and Baja California, *in* Zartman, R.E., ed., Short Papers of the Fourth International Conference, Geochronology, Cosmochronology, Isotope Geology: U.S. Geological Survey Open-File Report 78-701, p. 423–426.
Taylor, S.R., 1967, The origin and growth of continents: Tectonophysics, v. 4, no. 1, p. 17–34, doi:10.1016/0040-1951(67)90056-X.
Tepper, J.H., Nelson, B.K., Bergantz, G.W., and Irving, A.J., 1993, Petrology of the Chilliwack batholith, North Cascades, Washington: Generation of calc-alkaline granitoids by melting of mafic lower crust with variable water fugacity: Contributions to Mineralogy and Petrology, v. 113, p. 333–351, doi:10.1007/BF00286926.
Thomas, J.B., and Sinha, A.K., 1999, Field, geochemical, and isotopic evidence for magma mixing and assimilation and fractional crystallization processes in the Quottoon igneous complex, northwestern British Columbia and southeastern Alaska: Canadian Journal of Earth Sciences, v. 36, p. 819–831, doi:10.1139/e99-001.
Treuil, M., and Varet, J., 1973, Critères volcanologiques, pétrologiques et géochimiques de la genèse et de la différenciation des magmas basaltiques: Exemple de l'Afar: Bulletin de la Société Géologique de France, 7e Série, v. 15, no. 5–6, p. 506–540.
Tulloch, A.J., and Kimbrough, D.L., 2003, Paired plutonic belts in convergent margins and the development of high Sr/Y magmatism: Peninsular Ranges batholith of Baja-California and Median batholith of New Zealand, *in* Johnson, S.E., Paterson, S.R., Fletcher, J.M., Girty, G.H., Kimbrough, D.L., and Martín-Barajas, A., eds., Tectonic Evolution of Northwestern México and the Southwestern USA: Geological Society of America Special Paper 374, p. 275–295.
Vermeesch, P., 2006, Tectonic discrimination of basalts with classification trees: Geochimica et Cosmochimica Acta, v. 70, p. 1839–1848, doi:10.1016/j.gca.2005.12.016.
Vigneresse, J.L., and Tikoff, B., 1999, Strain partitioning during partial melting and crystallizing felsic magmas: Tectonophysics, v. 312, p. 117–132, doi:10.1016/S0040-1951(99)00167-5.
Wall, V.J., Clemens, J.D., and Clarke, D.B., 1987, Models for granitoid evolution and source compositions: The Journal of Geology, v. 95, no. 6, p. 731–749, doi:10.1086/629174.
Weaver, B.L., and Tarney, J., 1982, Andesitic magmatism and continental growth, *in* Thorpe, R.S., ed., Andesites: Orogenic Andesites and Related Rocks: New York, Wiley, p. 639–661.
Weaver, S.D., Sceal, J.S.C., and Gibson, I.L., 1972, Trace-element data relevant to the origin of trachytic and pantelleritic lavas in the East African Rift system: Contributions to Mineralogy and Petrology, v. 36, p. 181–194, doi:10.1007/BF00371430.
Wells, M.L., and Hoisch, T.D., 2008, The role of mantle delamination in widespread Late Cretaceous extension and magmatism in the Cordilleran orogen, western United States: Geological Society of America Bulletin, v. 120, no. 5/6, p. 515–530, doi:10.1130/B26006.1.
Whalen, J.B., Currie, K.L., and van Breemen, O., 1987, Episodic Ordovician-Silurian plutonism in the Topsails igneous terrane, western Newfoundland: Transactions of the Royal Society of Edinburgh–Earth Sciences, v. 78, p. 17–28, doi:10.1017/S0263593300010920.
White, W.M., and Dupré, B., 1986, Sediment subduction and magma genesis in the Lesser Antilles: Isotopic and trace element constraints: Journal of Geophysical Research, v. 91, no. B6, p. 5927–5941, doi:10.1029/JB091iB06p05927.
Whittington, A.G., Hofmeister, A.M., and Nabelek, P.I., 2009, Temperature-dependent thermal diffusivity of the Earth's crust and implications for magmatism: Nature, v. 458, p. 319–321, doi:10.1038/nature07818.
Wilcox, R.E., 1999, The idea of magma mixing: History of a struggle for acceptance: The Journal of Geology, v. 107, p. 421–432, doi:10.1086/314357.
Williams, R.W., and Gill, J.B., 1989, Effects of partial melting on the uranium decay series: Geochimica et Cosmochimica Acta, v. 53, p. 1607–1619, doi:10.1016/0016-7037(89)90242-1.
Wilson, M., 1989, Igneous Petrogenesis: London, Unwin Hyman, 466 p.
Wyllie, P.J., 1977, Crustal anatexis: An experimental study: Tectonophysics, v. 43, p. 41–71, doi:10.1016/0040-1951(77)90005-1.

MANUSCRIPT ACCEPTED BY THE SOCIETY 11 JUNE 2013